COLLOIDAL CHEMICAL POTENTIAL IN ATTRACTIVE NANOPARTICLE-POLYMER MIXTURES: SIMULATION AND MEMBRANE OSMOMETRY

A Thesis
Presented to
The Academic Faculty
By

Carlos A. Quant

In Partial Fulfillment
Of the Requirements for the Degree of
Master of Science in Chemical Engineering

School of Chemical and Biomolecular Engineering
Georgia Institute of Technology
August 16, 2004

COLLOIDAL CHEMICAL POTENTIAL IN ATTRACTIVE NANOPARTICLE-POLYMER MIXTURES: SIMULATION AND MEMBRANE OSMOMETRY

Approved by:

Dr. J Carson Meredith, Advisor

Dr. Athanasios Nenes

Dr. Peter Ludovice

August 16, 2004

In loving memory of my mother,

Jeannette,

Through her actions she showed me the true meaning of courage, faith, and strength and is now the inspiration for everything in my life.

ACKNOWLEDGEMENT

There are a lot of people I would like to thank for all their support throughout the course of this project. Without their time, effort, and encouragement, this endeavor would not have been possible. Most of all I would like to express gratitude to my Lord Jesus Christ who continues to make the impossible possible.

I would like to thank my advisor, Dr. J. Carson Meredith, whose confidence in my abilities has been unwavering and whose help has made this a solid project. His patience and dedication to helping me succeed is greatly appreciated. I am thankful to Dr. Nenes and Dr. Ludovice for taking the time to serve in my committee.

Throughout the course of my studies, the friendship and camaraderie offered by my friends, fellow graduate students, and the advanced polymer thin films and colloid materials research group has been indispensable and has made this learning experience enjoyable and relatively painless. I am grateful for the relationships that I have built with them. In particular, I would like to thank Krishna Marla for all his guidance and help with simulations as we mutually engaged in making sense of the obstacles and results encountered throughout the course of this project.

I am forever in debt to Gina, my wife, without her love, understanding, and companionship I wouldn't have been able to put forth my best effort and maintain my sanity. I am eternally grateful to Carlos, my father, whose unconditional support opened the doors to this journey called higher education. Finally, I would like to thank my

brother, Alberto, whose patient character and exemplary behavior has always inspired me to do the same.

TABLE OF CONTENTS

Acknowledgement . . . . . **iv**

List of Tables . . . . . **viii**

List of Figures . . . . . **ix**

Summary . . . . . **xi**

Chapter I Introduction **1**

1.1 Goals and Motivation 1

1.2 Thesis Outline 5

Chapter II Expanded Ensemble Monte Carlo Simulation of Attractive Nanocolloid-Polymer Mixtures: Comparison to a Modified Perturbed Lennard-Jones Equation of State **6**

2.1 Introduction 7

2.2 System Description, Simulation Methodology and PLJC Equation of State 9

2.2.1 Nanocolloidal Particle in the Presence of Freely Adsorbing Polymer Solution. 9

2.2.2 Expanded Ensemble Monte Carlo Simulation Methodology . 12

2.2.3 PLJC Equation of State for Nanocolloid and Polymer Mixtures 14

2.3 Results and Discussion 19

2.3.1 Effects of Polymer Density on Chemical Potential and Polymer Adsorption 19

2.3.2 Effects of Particle Diameter on Chemical Potential and Adsorption. 21

2.3.3 PLJC EOS vs. EEMC Simulation Results – Parameter ν_p . 23

2.3.4 Correction for Adsorption Effects. 26

2.3.5 Fit to Experimental Data. 29

2.4 Conclusions 31

Chapter III Measurement of Organically-Modified Nanoparticle Chemical Potentials using Osmometry 33

3.1 Introduction 34

3.2 Theory 36

3.2.1 Osmotic Pressure and Chemical Potential . . . 36

3.2.2 Chemical Potentials from Expanded Ensemble Monte Carlo Simulation 39

3.3 Experimental Section 40

3.3.1 Materials and Sample Preparation 40

3.3.2 Experimental Apparatus and Methodology . . . 41

3.4 Results and Discussion 43

3.4.1 Effects of Silica Concentration 43

3.4.2 Effects of poly(ethylene oxide) Concentration . . . 46

3.4.3 Effects of Temperature 50

3.5 Conclusions 51

Chapter IV Conclusions 52

References 56

LIST OF TABLES

2.1 Reduced polymer concentration (c_p/c_p^*) and radius of gyration (R_g) for different polymer segment densities and chain lengths studied for the EEMC simulations. 14

2.2 Corrected reduced chemical potential (μ^*), adsorption correction (μ^*_{cp}), and the constant C for different values of ε_{cp} and σ_c studied. 28

2.3 Result of the modified PLJC empirical parameters calculated from the regression analyses between EOS prediction and membrane osmometry experiments. 30

3.1 Osmotic pressure results for different PEO concentrations and at different temperatures. 49

LIST OF FIGURES

2.1 Infinite dilute reduced particle chemical potential ($\mu^* = \beta\mu$) vs. polymer segment density (ρ_p) at different chain lengths (n) for $\sigma_c = 10$. The solid markers (■) represent different values of simulation data and the solid lines (—) represent the PLJC EOS. 20

2.2 Absolute Adsorption per surface area of the particle (Γ_s) vs. polymer segment density (ρ_p) at different chain lengths (n) for $\sigma_c = 10$. The markers represent different values of simulation data. 21

2.3 Infinite dilute reduced particle chemical potential ($\mu^* = \beta\mu$) vs. colloid diameter (σ_c) at three different polymer segment densities (ρ_p) for $n = 10$. The markers represent EEMC simulation data at polymer segment densities of 0.10, 0.16, and 0.20, the solid line (——) represents the PLJC equation of state extended to nanocolloid-polymer mixtures. 22

2.4 Excess amount adsorbed per unit surface (Γ^{ex}_s) and excess amount adsorbed (Γ^{ex}) vs. colloid diameter (σ_c) at different polymer segment densities (ρ_p) for $n = 10$. The markers represent different values of simulation data. The lines are a visual aid. 23

2.5 Log-log plot of the empirical parameter ν_p vs. chain length (n) at different polymer segment densities (ρ_p). The markers represent the ν_p calculated by using the regression procedure outlined previously. The lines are power-law regressions. 25

2.6 Average ($\nu_p \cdot R_g^x \cdot m \cdot n$) vs. polymer segment densities (ρ_p) using data for all chain lengths (n). The markers represent averages calculated by using the regression procedure mentioned above, where $x = {}^5/_3$. The error bars represent 95% confidence intervals. Error bars that were smaller than the markers representing the data have been omitted. 26

2.7 Infinite dilution colloid chemical potential (μ^*) vs. colloid diameter (σ_c) at different interaction energies (ε_{cp}) for $n = 10$. The markers represent EEMC simulation data at ε_{cp} of 0.05 and 0.25, where the square markers (□) represent $\varepsilon_{cp} = 0.05$ and the circular markers (○) represent $\varepsilon_{cp} = 0.25$. The solid lines (—) represent the mPLJC equation of state with the inclusion of the correction term, and the dotted lines represent the PLJC without the

correction (····) for ε_{cp} = 0.05 and (- - -) for ε_{cp} = 0.25.. . . . 28

2.8 Reduced colloid chemical potential ($\mu^*=\mu/kT$ (PLJC) or $\mu^*=\mu \cdot M_w/RT$ *(experiment))* vs. silica volume fraction (v_{si}) at different PEO mass %. The markers represent membrane osmometry data, where the triangular markers (Δ) represent PEO mass % = 2, the square markers (□) represent PEO mass % = 5, and the circular markers (○) represent PEO mass % = 7. The solid line (▬) represent the modified PLJC equation of state for 7 mass % PEO, and the dotted lines represent the modified PLJC (····) for 5 mass % PEO and (- - -) 2 mass % PEO. The error bars shown are 95% confidence intervals. 31

3.1 A schematic diagram of the three component system in this study. The ● represents the nanocolloid, ⸙ represents the polymer. . . . 36

3.2 Reduced particle chemical potential ($\mu^* = \mu \cdot M_w /RT$) as a function of silica mass % for 5 mass % PEO. The markers denote the average value of multiple experimental runs under constant conditions and the error bars shown are 95% confidence intervals. 43

3.3 Reduced particle chemical potential ($\mu^* = \mu \cdot M_w /RT$) as a function of silica volume fraction (v_{si}) for different PEO mass %. The markers denote the actual osmometric measurements and the dotted lines are used merely as a visual aid. 45

3.4 EEMC simulation reduced particle chemical potential ($\mu^* = \mu/kT$) as a function of colloid volume fraction (v_c) for different polymer volume fractions (v_p). The colloids have a diameter σ_c = 5 σ_p, where σ_p is the diameter of a polymer chain segment and the polymer chain length (n) = 30. The markers denote the actual EEMC simulation results, the lines are used merely as a visual aid.. 45

3.5 Reduced particle chemical potential ($\mu^*=\mu \cdot M_w /RT$) as a function PEO volume fraction (v_{PEO}) for different mass % SiO_2. The markers denote the actual osmometry measurements and the lines are used merely as a visual aid. 48

3.6 EEMC simulation reduced particle chemical potential ($\mu^* = \mu/kT$) as a function of polymer segment volume fraction (v_p) for different chain lengths (n). The markers denote the actual simulation results, the lines are used merely as a visual aid. 48

3.7 Reduced particle chemical potential ($\mu^*=\mu \cdot M_w /RT$) as a function of mass % SiO_2 for 5% mass % PEO at different temperatures. The markers denote the actual osmometric measurements and the lines are used merely as a visual aid. 50

SUMMARY

The potential applications of dispersed and self-assembled nanoparticles depend critically on accurate control and prediction of their phase behavior. The chemical potential is essential in describing the equilibrium distribution of all components present in every phase of a system and is useful as a building block for constructing phase diagrams. Furthermore, the chemical potential is a sensitive indicator of the local environment of a molecule or particle and is defined in a mathematically rigorous manner in both classical and statistical thermodynamics. The goal of this research is to use simulations and experiments to understand how particle size and composition affect the particle chemical potential of attractive nanoparticle-polymer mixtures.

The expanded ensemble Monte Carlo (EEMC) simulation method for the calculation of the particle chemical potential for a nanocolloid in a freely adsorbing polymer solution is extended to concentrated polymer mixtures. The dependence of the particle chemical potential and polymer adsorption on the polymer concentration and particle diameter are presented. The perturbed Lennard-Jones chain (PLJC) equation of state (EOS) for polymer chains[1] is adapted to calculate the particle chemical potential of nanocolloid-polymer mixtures. The adapted PLJC equation is able to predict the EEMC simulation results of the particle chemical potential by introducing an additional parameter that reduces the effects of polymer adsorption and the effective size of the colloidal particle.

Osmotic pressure measurements are used to calculate the chemical potential of nanocolloidal silica in an aqueous poly(ethylene oxide) (PEO) solution at different silica and PEO concentrations. The experimental data was compared with results calculated from Expanded Ensemble Monte Carlo (EEMC) simulations. The results agree qualitatively with the experimentally observed chemical potential trends and illustrate the experimentally-observed dependence of the chemical potential on the composition. Furthermore, as is the case with the EEMC simulations, polymer adsorption was found to play the most significant role in determining the chemical potential trends.

The simulation and experimental results illustrate the relative importance of the particle's size and composition as well as the polymer concentration on the particle chemical potential. Furthermore, a method for using osmometry to measure chemical potential of nanoparticles in a nanocolloid-mixture is presented that could be combined with simulation and theoretical efforts to develop accurate equations of state and phase behavior predictions. Finally, an equation of state originally developed for polymer liquid-liquid equilibria (LLE) was demonstrated to be effective in predicting nanoparticle chemical potential behavior observed in the EEMC simulations of particle-polymer mixtures.

CHAPTER I

INTRODUCTION

1.1 Goals and Motivation

Nanotechnology is an interdisciplinary area of active research that has the potential to enable the rational design, at the molecular level, of materials with novel physical and chemical characteristics. Nanoscale materials display unique optical, electronic, chemical, and mechanical properties not found on their bulk counterparts that depend sensitively on the particle size and composition. Current research has been focused primarily on discovering suitable ways to use self-assembly to fabricate functional materials in a controlled, predictable, and repeatable manner. Colloidal nanoparticles, "nanocolloids", are commonly used for assembly of ordered structures. Since most nanoparticles are unstable in dispersions,[2] polymers and oligomers have been widely used as stabilizing agents to promote organized self-assembly and avoid uncontrolled flocculation.[3] The physical and chemical properties (chain length, polymer adsorption, polymer type) of these stabilizing agents could be tailored to adjust the stability of colloidal dispersions. Experiments that report controlled studies of nanoparticles stability as a function of modifier properties or measurements of fundamental thermodynamic quantities are scarce. In addition, the lack of robust molecular models to guide interpretation of experimental results is a great obstacle for the

design of appropriate nanoparticles stabilizers. Several organically modified nanocolloid systems recently studied include self-assembled nanocolloid silica particles grafted with polystyrene-poly(benzyl acrylate) block copolymer chains,[4] self-assembled multidimensional structures of metal nanocrystals with the aid of alkane thiols,[5,6] synthesis of Pd nanoparticles stabilized with poly(vinylpyrrolidone),[7] and gold nanocolloids organized in the presence of sodium mercaptoacetate.[8]

Numerous theoretical[9-15] and simulation[16,17] published studies of nanocolloids in non-adsorbing polymer solutions aim to develop molecular based approaches that relate the particle size, modifier length, and component composition to the nanocolloid mixture phase behavior. One of the shortcomings of these investigations is the use of hard sphere models to describe the polymer and colloid mixtures since many processes involved in self-assembly and colloid stability involve organically-modified nanoparticle systems that have particle-polymer attractive interactions. Although there have been some published studies[18,19] of attractive nanoparticles-polymer systems, current research in this area is still limited. One of the biggest obstacles in studying attractive nanoparticles-polymer systems is that the interfacial free energy of the colloidal particle is dependent on the extent of polymer adsorption and the polymer chain conformations. A relatively new application of the expanded ensemble Monte Carlo method adapted to calculate efficiently the particle chemical potential of nanocolloid dispersed in a freely-adsorbing dilute polymer solution has been developed.[18] By extending this method outside the dilute polymer concentration regime, this investigation seeks to understand how polymer density, chain length, and colloid size affect the chemical potential and polymer adsorption in order to develop thermodynamic chemical potential models that could be

used to calculate and predict the phase behavior of dispersed and self-assembled nanoparticles. These chemical potential models are essential to the development of the potential applications in nanotechnology. The sensitivity of the particle chemical potential to the local molecular environment and particularly to polymer adsorption was also observed in the simulations at higher polymer concentrations. In addition, the observed trends at higher polymer concentrations show the chemical potential dependence on the particle size and chain length does not change with increasing polymer concentration.

Although great technological advances have been made in terms of computer speed and power, molecular simulations are still costly and time consuming. An equation of state (EOS) that could predict accurately the thermodynamic behavior of nanoparticle-polymer systems would be an attractive alternative to simulations. In addition, very few molecular models and EOS for attractive nanocolloid-polymer mixtures have been developed. However, extensive research has been devoted to the development of analytical EOS for polymer chain molecules.[20-27] For this reason, a perturbed Lennard-Jones chain (PLJC) EOS[1] developed for polymer mixtures with application in liquid-liquid equilibria (LLE) was used as a basis to propose a modified PLJC EOS with applications for nanoparticles-polymer mixtures that could be used to predict phase behavior. The PLJC EOS uses a hard-sphere equation as a reference system representing repulsive interactions and a first-order variational perturbation term accounting for the attractive interactions. The PLJC model compares to the EEMC simulation model[18] in that the chains consist of freely jointed tangential Lennard-Jones segments and both models are characterized by three independent parameters chain length (n), interaction

energy (ε), and segment size (σ).[1,28,29] The PLJC EOS was extended for polymer chains and colloidal particles without accounting explicitly for the solvent molecules similar to the EEMC simulations.[18] The prediction of the modified PLJC EOS for nanoparticles-polymer mixtures compare particularly well to the trends observed in the EEMC simulations.

Even though various experimental studies investigating the interactions in attractive polymer-particle-surfactants systems[30,31] and the effects of adsorption of poly-ethylene-oxide (PEO) on silica[32-35] have been performed, these studies have focused on phenomena that indirectly depend on the particle and polymer chemical potentials, such as osmotic compressibility and adsorption. To our knowledge, no experimental measurements have been reported that relate directly the colloid chemical potential with the particle and polymer molecular properties and concentration. A main objective of this research is to devise a technique to experimentally measure chemical potential to complement simulation and theoretical efforts in developing accurate chemical potential models for nanocolloid-polymer systems. Membrane osmometry is used to measure the chemical potentials of silica nanoparticles in an aqueous PEO solution. The observed experimental trends are compared to the results of the EEMC simulation. The experimental and simulation trends agree qualitatively very well. This new application of membrane osmometry for measuring chemical potentials could be an important step to developing appropriate chemical potential models that can be used to predict phase behavior and to develop EOS for attractive nanoparticles-polymer systems.

1.2 Thesis Outline

The remaining part of this thesis is composed of two journal papers that have been submitted for publication, therefore some explanations and descriptions of the techniques and models utilized in this work may be repeated and expressed in various locations throughout the thesis. The remainder of the thesis is organized as follows: In Chapter II, the investigation using EEMC simulations at higher polymer concentrations that includes a brief description of the attractive nanoparticles-polymer model system, the EEMC simulation details and methodology are described. This chapter provides a detailed description of the development of the modified PLJC EOS and comparisons of the EEMC and EOS results which were found to be in good agreement. Chapter III shows the results of the experimental study that uses membrane osmometry to measure particle chemical potentials and provides a comparison with EEMC simulation results. Theoretical arguments that relate the osmotic pressure to the particle chemical potential are given as well as the experimental details including materials, sample preparation, and experimental methodology. The observed experimental trends were compared to the EEMC simulation results, with good qualitative agreement. Concluding remarks and proposed future research studies are described in Chapter IV.

CHAPTER II

EXPANDED ENSEMBLE MONTE CARLO SIMULATION OF ATTRACTIVE NANOCOLLOID-POLYMER MIXTURES: COMPARISON TO A MODIFIED PERTURBED LENNARD-JONES EQUATION OF STATE

The development of predictive equations of state for nanoparticle-surfactant and polymer mixtures is of extreme importance in nanotechnology and fabrication of advanced materials. In this chapter, the perturbed Lennard-Jones chain (PLJC) equation of state (EOS)[1] for polymer solutions is modified and extended to calculate the chemical potentials in nanocolloid-polymer mixtures. The EOS predictions are compared to Monte Carlo simulations that use the same LJ molecular model. The PLJC equation predicts the simulation nanoparticle chemical potential as a function of particle and polymer concentrations, and particle diameter for *symmetric* polymer and colloid LJ energy parameters. This corresponds to strong polymer adsorption on the nanoparticles. When the colloid-polymer attraction differs significantly from the polymer-polymer attraction (weak adsorption), the PLJC must be further modified to obtain good agreement with simulations. The PLJC is modified by introducing a semi-empirical parameter that accounts for the effects of weak polymer adsorption and size differences on free energy.

2.1 Introduction

Nanotechnology is an interdisciplinary area of research that has recently emerged as one of the most promising areas of scientific study because of its potential to revolutionize the synthesis and processing of materials. Nanoscale materials display exceptional physical and chemical characteristics that depend sensitively on the particle size and composition. Much research has been focused on discovering suitable ways to use self-assembly to fabricate and organize colloidal nanoparticles efficiently and reliably into practical materials. In many cases polymers and oligomers are widely used in suspensions to stabilize colloidal particles to avoid flocculation and guide self-assembly. Variations in the modifier chain length, adsorption, and chemistry can be used to control the stability of colloidal dispersions.[36] Recent examples include nanocolloid silica particles grafted with polystyrene-poly(benzyl acrylate) block copolymer chains,[4] self-assembled multidimensional structures of metal nanocrystals with the aid of alkane thiols,[5,6] and Pd nanoparticles synthesized by stabilization with poly(vinylpyrrolidone).[7] Unfortunately, robust models for predicting the effects of stabilizers on nanoparticle dispersions are not available, particularly for systems that involve attractions.

Thermodynamic chemical potential models that can be used to predict the phase behavior of nanoparticles-polymer mixtures are essential to nanotechnology. The chemical potential is an important thermodynamic property that is defined in a mathematically rigorous manner in both classical and statistical thermodynamics. In addition, the chemical potential can provide valuable information of the local environment of a molecule or particle. The measurement and prediction of chemical potentials for nanoparticles is not well developed, especially in the case of *attractive*

systems, where polymer and particles interact with attraction. There have been a number of theoretical,[16,17] experimental,[37] and simulation[9-14,38] studies of the effects of polymer-nanocolloid systems (this list is by no means exhaustive). Most have focused primarily on *hard sphere repulsive systems* that do not account for particle-polymer attraction. Recently, the expanded ensemble Monte Carlo (EEMC)[39-41] technique was adapted to calculate efficiently the *infinite dilution* chemical potential of nanoparticles[42] dispersed with freely adsorbing polymers (attractive) for dilute polymer concentrations.[18] Molecular-based simulation approaches allow a semi-quantitative description of the dependence of the chemical potential (and other properties) on size and structure of the polymer and colloidal particle.

The effect of the polymeric surfactant and colloid concentrations on the particle chemical potential must be understood prior to modeling colloidal self-assembly, which often occurs at volume fractions exceeding 50% for hard-spheres. For this purpose, the EEMC method was extended to higher polymer concentration approaching the semidilute crossover concentration. The results, as we shall describe below, verified that the trends for the dilute polymer regime, published recently,[18] do not change at higher (semidilute) polymer concentrations. Moreover, the simulation results provide a well-defined system to which models can be validated.

Although, few robust models or equations of state (EOS) for attractive nanocolloid-polymer mixtures have been developed, extensive research and effort has been centered on developing an analytical EOS for polymer solutions.[20-27] In this chapter, we investigate the use of one particular polymer EOS, the perturbed Lennard-Jones chain (PLJC) EOS,[1] by extending it to nanocolloid-polymer mixtures.

Furthermore, we investigate its use as a foundation for a "modified" PLJC EOS that accounts for the effects of weak polymer adsorption and size differences on free energy. The PLJC is based on a first-order variational perturbation for attractive Lennard-Jones (LJ) chains[28,29] that uses a hard-sphere reference system[43] to represent repulsive interactions. The PLJC model consists of freely jointed tangential LJ segments[28,29] and is characterized by three independent parameters: chain length (n), interaction energy (ε), and segment size (σ_i).[1] The same parameters are used in the EEMC simulations of Lennard-Jones polymer-colloid mixtures, providing a basis for comparing the two results.[18] Since the PLJC was developed originally for polymer liquid-liquid equilibria (LLE), we expect regimes where it fails to predict colloid-polymer properties. The remaining parts of this chapter are organized as follows: In section 2.2, a brief description of the model system and EEMC simulation details is given. This section also includes the original PLJC equation[1] extended to polymer-nanocolloid mixtures and our modifications to account for asymmetric polymer and colloid LJ energy parameters. Section 2.3 presents and discusses the comparison between EEMC simulations, the PLJC EOS extended for nanocolloid-polymer mixtures, and the modified PLJC (mPLJC) EOS, followed by the concluding remarks in Section 2.4.

2.2 System Description, Simulation Methodology and PLJC Equation of State

2.2.1 Nanocolloidal Particle in the Presence of Freely Adsorbing Polymer Solution

The Expanded Ensemble Monte Carlo (EEMC) method[39,44] was applied to a system consisting of a single nanocolloidal particle in a dispersion of freely adsorbing

fully-flexible polymer chains in a continuum solvent. We calculated the particle and polymer chain chemical potentials and the polymer adsorption as a function of the chain length (n), colloid diameter (σ_c), and polymer segment density (ρ_p = number of segments / box volume), where volume is in units of the polymer segment diameter, σ_c^3. The chain lengths in the polymer solution were varied from sizes n = 5 to n = 30. The effects of polymer segment density with reference to the work by Marla and Meredith[18] was also investigated at higher polymer segment number densities where ρ_p = 0.16, 0.18, 0.20, 0.25, and 0.30. These polymer densities correspond to a range of c_p/c_p^* (polymer molar concentration: polymer semidilute crossover concentration ratio) of 0.15 to 0.78. This investigation studied the effects of varying the colloid particle diameter (σ_c) over $1\sigma_p \leq \sigma_c \leq 10\sigma_p$, on the particle chemical potential (μ_c). The system was held at a constant reduced temperature, T^* = 3.0, which has been shown to reproduce good solvent conditions for bulk solutions and to be above the theta T^* of 2.5 for this Lennard-Jones polymer model.[45]

The polymer chains are represented by using the self-avoiding random walk model in a good solvent. The chains are made up of freely-jointed tangential Lennard-Jones spherical segments with bond length σ_p. The nanocolloid was modeled as an LJ sphere with diameter σ_c. The solvent molecules are not explicitly accounted for in the simulation but one can vary the reduced temperature (T^*), therefore reducing the relative contribution of the attractive and repulsive interactions, to simulate the effects of different types of solvents.

Two types of interactions were taken into account: non-bonded polymer segment-segment interaction and polymer segment-colloid interaction. In order to achieve

efficiency in the calculation of energies and because the calculation of the non-bonded energies requires the greatest computational effort, the polymer segment-segment interactions were modeled using a truncated 6-12 Lennard-Jones potential where the force and energy are zero at $r_c \geq 2.5 \cdot \sigma_p$ as described by Marla and Meredith.[18] The model of the LJ potential cutoff is shown in eq. (2.1),[18]

$$u(r_{ij}) = \begin{cases} 4\varepsilon_{ij}\left[\left(\frac{\sigma_{ij}}{r_{ij}}\right)^{12} - \left(\frac{\sigma_{ij}}{r_{ij}}\right)^{6} - \left(\frac{\sigma_{ij}}{r_c}\right)^{12} + \left(\frac{\sigma_{ij}}{r_c}\right)^{6}\right] & r > r_c \\ 0 & r \leq r_c \end{cases} \qquad (2.1)$$

where r is the distance between interacting sites in the simulation, ε_{ij} is the energy interaction parameter, and $\sigma_{ij} = \frac{1}{2}(\sigma_i + \sigma_j)$ is the size parameter. For the polymer segment – colloid interactions the full LJ potential with no cutoff was used since no considerable reduction in computational effort would be gained from a cut-off potential. It should be noted that the 6-12 LJ potential is not an experimentally realistic model for the system at hand due to the fact that this potential was derived for point-point interactions. For the colloid-polymer interaction, an integration of the LJ potential for each of the atoms that make up the colloid and each polymer segment would be a better approximation. It has been shown that such an integration would result in a potential proportional to $\sim \{(\sigma/r)^9 - (\sigma/r)^3\}$.[46,47] The LJ point model does, however, capture some of the essential physics of van der Waals dispersion interactions.[18]

2.2.2 Expanded Ensemble Monte Carlo Simulation Methodology

The EEMC method is employed to calculate the excess chemical potential of the colloidal particle and of the polymer chains. To ensure the system achieves thermal equilibrium random translation and displacement of the colloid and chain segments are attempted and accepted according to the standard Metropolis Monte Carlo[48] criterion (colloid) or the continuum configurational bias (CCB)[38,49] criterion (polymer).

All simulations were performed using periodic boundary conditions in a cube with length, $l = 40\sigma_p$, in order to avoid any self interaction through the periodic boundaries.[18] The reduced variables used in the simulation are: $T^* = T \cdot k_B / \varepsilon_{ss}$, $\rho_p^* = \rho_p \cdot \sigma_p^3$, and $\rho_p = M \cdot n / V$; where T is the temperature, k_b is the Boltzmann constant, ε_{ss} is the segment-segment interaction energy, M is the number of chains, and V is the volume of the simulation box. A general overview of the method will be described below; a more complete and detailed description can be found elsewhere.[39-42,50] The expanded ensemble method (EE) calculates chemical potentials by using additional ensemble variables[39,44,51] that are adjusted to define a smooth and reversible path for the measurement of the free energy between different states of the system.[40,41,50] In the case of the particle chemical potential, the additional expansion variable is the diameter of the colloidal particle. The EE method applied to the calculation of colloid particle chemical potential has been shown[18] to increase the efficiency at which the particle chemical potential is calculated and avoids the uncertainties and steric overlaps of other particle insertion methods such as the Widom[52] and inverse-Widom.[53] The simulation calculates the incremental particle chemical potential, $(\beta\mu^{ex}_c)$, at each predetermined colloidal diameter increment by eq. (2.2),[18]

$$\beta\mu_c^{ex} = -\ln\left[\exp\left(\frac{-\Delta E}{k_B T}\right)\right] \tag{2.2}$$

where ΔE is the energy change in the system due to the increment in the colloidal diameter. Each increment or decrement is accepted or rejected using an acceptance criterion similar to Metropolis.[48] The sum of all the incremental $\beta\mu^{ex}{}_c$ gives the full size particle $\beta\mu^{ex}{}_c$. Since the method for calculating the particle and the chain chemical potential are similar, the reader is referred to recent publications by Escobedo and de Pablo[38,39,44,54] for the details of the calculation of the chemical potential for polymer chains using the EE method. As was mentioned earlier, the CCB algorithm is used to perform chain displacements by re-growing a predetermined part of the chain into a lower energy conformation while avoiding overlaps with neighboring chains segments and with the colloidal particle. A more rigorous treatment of the CCB method is shown in references.[49,55,56] Absolute adsorption of chain segments per unit surface area of the colloidal particle was also calculated by integration of the segment density profile near the particle surface. A detailed description of this procedure is shown in Ref 18.

To obtain statistically significant results for the variables studied (R_g, $\beta\mu^{ex}{}_c$, etc.) the simulations were averaged over 100-200 x 10^6 steps, where one step corresponds to one attempted move. As was shown in Ref 18, twenty percent of the total moves attempted were colloid moves divided equally, that is 10% metropolis-type colloid displacement and 10% colloid EE moves. The remaining steps were chain moves divided equally between EE and CCB moves. Table 1 shows the polymer radius of gyration (R_g)

and the reduced polymer concentration ($c_p/c_p^* = {}^4/_3 \cdot {}^\pi/_n \cdot \rho_p \cdot R_g^3$) for all the system conditions studied in this investigation. Statistical analysis based on the inefficiency parameter[57] was performed on the simulation results and are presented in the Results and Discussion section.

Table 2.1 - Reduced polymer concentration (c_p/c_p^*) and radius of gyration (R_g) for different polymer segment densities and chain lengths studied for the EEMC simulations.

	ρ_p	R_g	$c_p/c_p^* = {}^4/_3 \cdot {}^\pi/_n \cdot \rho_p \cdot R_g^3$
n = 5	0.18	1.0017	0.1476
	0.20	1.0016	0.1684
	0.25	1.0011	0.2059
	0.30	0.9983	0.2540
	0.35	0.9942	0.2881
n = 10	0.16	1.5636	0.2598
	0.18	1.5618	0.2804
	0.20	1.5609	0.3186
	0.25	1.5592	0.3869
n = 20	0.18	2.3632	0.4862
	0.20	2.3621	0.5517
	0.25	2.3580	0.6697
n = 30	0.16	2.9810	0.6007
	0.18	2.9980	0.6621
	0.20	3.0188	0.7788

2.2.3 PLJC Equation of State for Nanocolloid and Polymer Mixtures

Extensive research has centered on deriving analytical equations of state (EOS) for polymers and their solutions.[20-27] Recently Lee et al.[1] derived a perturbation theory EOS with applications for polymer-polymer and polymer-solvent liquid-liquid equilibria, known as the perturbed Lennard-Jones chain EOS. Since very few robust models and

EOS for attractive nanocolloid-polymer systems exist, and since the PLJC molecular model matches our simulation *exactly*, we used the PLJC as the foundation to propose a polymer-colloid EOS. This provides an unusual opportunity to compare EOS predictions to simulation results.

The PLJC's treatment of the polymer chain is similar to the EEMC simulation's treatment[18] where the chains are made up of freely-jointed tangential LJ segments with bond length σ_p. The solvent molecules are treated as spherical LJ particles with size σ_s. The PLJC has three characteristic parameters equivalent to those used in the EEMC simulations: the chain length (n), the segmental interaction energy (ε_{ij}), and the segment size (σ_i) that are comparable to the MC simulation parameters. Details of the derivation of the PLJC for polymer mixtures and polymer-solvent systems are shown elsewhere.[1,27-29,58] A summary of the method is described below. The PLJC is composed of two parts: one is a hard sphere chain model used as a convenient reference system and the other is a perturbation term derived from perturbation or variational theories. The excess Helmholtz energy A_{mixt} for the colloid-polymer mixture is shown below:[1]

$$\frac{A_{mixt}}{N_c k_B T} = \frac{A_{mixt}^{HSC}}{N_c k_B T} + \frac{A_{mixt}^{PERT}}{N_c k_B T} \tag{2.3}$$

where N_c is the sum of the number of polymer segments and colloidal particles. The excess Helmholtz energy for the hard sphere reference is defined as:[29]

$$A_{mixt}^{HSC} = N_c k_B T * \left[\left(\frac{\zeta_2^3}{\zeta_0 \zeta_3^2} - 1 \right) \ln(1-\zeta_3) + \frac{3\zeta_1\zeta_2}{\zeta_0(1-\zeta_3)} + \frac{\zeta_2^3}{\zeta_0\zeta_3(1-\zeta_3)^2} \right]$$

$$+ \phi_{cc} \left(1 - \frac{1}{n_c} \right) \left[\ln(1-\zeta_3) - \frac{3\zeta_1 d_{cc}}{2(1-\zeta_3)} \right] + \phi_{pp} \left(1 - \frac{1}{n_p} \right) \left[\ln(1-\zeta_3) - \frac{3\zeta_1 d_{pp}}{2(1-\zeta_3)} \right] \qquad (2.4)$$

where,

$$\zeta_j = \frac{\pi}{6} \sum_i n_i \rho_c d_{ii}^j \qquad (2.5)$$

$$\phi_{ii} = \frac{x_i n_i}{\sum_j x_j n_j} \qquad (2.6)$$

$$\left(\frac{2^{1/6}}{a_{ii}} - 1 \right)^3 = \left(\frac{0.005397 n_i + 0.006354}{9.44 + n_i} \right) \cdot T^* + \left(\frac{0.01222 n_i + 0.005102}{9.947 + n_i} \right) \qquad (2.7)$$

n_i is either the number of segments the make up the polymer chain length (n_p) or colloid (n_c). n_c = 1, since the number of segments that make up a colloid is one. x_i is the fraction of chain segments or colloid particles in the system, ρ_c is the chain number density, and d_{ii} ($d_{ii} = a_{ii} \cdot \sigma_{ii}$) is the optimal dimensionless diameter of a hard-sphere segment obtained from numerical minimization of the free energy of the system which is then fitted to the expression shown in eq. (2.7).[27]

From a variational first order perturbation theory, von Solms et al.[29] derived the attractive (perturbation) term as shown in eq. (2.8) which has been modified with minor changes to reflect the colloid – polymer system at hand.

$$A_{mixt}^{PERT} = 2\pi\rho_c N_c \varepsilon_{cc}\left\{\phi_c^2 n_c^2\left(\frac{\sigma_{cc}}{a_{cc}}\right)^3\left[I_{A_{cc}} + I_{B_{cc}}\left(\frac{1}{a_{cc}^6}-1\right)\right]\right\} \tag{2.8}$$

$$+\phi_c\phi_p n_c n_p \upsilon_p \frac{\varepsilon_{cp}}{\varepsilon_{cc}}\left(\frac{\sigma_{cp}}{a_{cp}}\right)^3\left[I_{A_{cp}} + I_{B_{cp}}\left(\frac{1}{a_{cp}^6}-1\right)\right]$$

$$+\phi_p^2 n_p^2 \upsilon_p^2 \frac{\varepsilon_{pp}}{\varepsilon_{cc}}\left(\frac{\sigma_{pp}}{a_{pp}}\right)^3\left[I_{A_{pp}} + I_{B_{pp}}\left(\frac{1}{a_{pp}^6}-1\right)\right]$$

where ν_p is an empirical parameter that will be discussed later and I_{Aii} and I_{Bii} are perturbation integrals which have been fitted to analytical expressions as shown in eqs. (2.9) and (2.10).[1,27]

$$I_{A_{ii}} = \frac{(-0.22169 n_i - 1.0755) - (2.2618 n_i - 1.0385)\zeta_3 + (1.47 n_i - 0.55411)\zeta_3^{\,2}}{0.4571 + n_i} \tag{2.9}$$

$$I_{B_{ii}} = \left(0.03171 + \frac{0.4213}{n_i}\right) + \left(0.66264 + \frac{0.0987}{n_i}\right)\zeta_3 + 1.7866\zeta_3^{\,2} \tag{2.10}$$

The average between the polymer-polymer and colloid-colloid parameters (such that M_{ij} =½ $\{M_{ii} + M_{jj}\}$) was used as the mixing rule for ρ_{ij}, d_{ij}, I_{Aij}, $I_{Bij.}$ For the ε_{ij} and a_{ij} the following mixing rules were used: $\varepsilon_{cp} = \sqrt{\varepsilon_{cc}\varepsilon_{pp}}$ and $a_{cp} = (a_{pp}\sigma_{pp} + a_{cc}\sigma_{cc})/(\sigma_{pp} + \sigma_{cc})$.

The governing equation that relates the Helmholtz free energy to the chemical potential is eq. (2.11). Due to the cumbersome nature of deriving an analytical solution to eq. (2.11), a numerical method approach was chosen instead. The forward finite-divided-difference (FFDD) numerical differentiation technique was used to evaluate eq. (2.11).

Since the infinite particle dilution ($\beta\mu_c$) is to be calculated, the central finite-divided-difference (CFDD) or the backward finite-divided-difference (BFDD) could not be employed since they require data points outside the available range. Eq. (2.12) shows the FFDD formula used, where h is the step size.

$$\beta\mu_c = \left.\frac{\partial A_{mixed}}{\partial n_c}\right|_{n_p,T,V} \tag{2.11}$$

$$f'(x_i) = \frac{-f(x_{i+2}) + 4f(x_{i+1}) - 3f(x_i)}{2h} \tag{2.12}$$

The empirical parameter ν_p (from eq. (2.8)), introduced by Hino et al. [59] for a perturbed hard-sphere-chain EOS and further extended by Lee et al.[1] for the PLJC, has been used successfully to predict LLE behavior of various polymeric systems. This empirical term arises from the fact that the perturbation term in the model over-predicts the attractive interaction between polymer chains. Hence, without the modification the PLJC incorrectly predicts phase separation under conditions where phases should be stable.[1] Due to the similarity between models (colloid-polymer system and solvent-polymer system), an analogous empirical parameter can be used in the EOS for the colloid-polymer system. The regression procedure described by Lee et al.[1] was adopted in this study to use the PLJC to model a nanocolloid and polymer surfactant mixture by adjusting the empirical parameter ν_p. The objective function of the regression was

chosen to be the sum of squared error (SSE) between the calculated particle chemical potentials ($\beta\mu_{calc}$) and the EEMC simulation ($\beta\mu_{mc}$) and is shown in eq. (2.13)

$$SSE = \sum_{i=1}^{d} \left(\frac{\beta\mu_{calc} - \beta\mu_{mc}}{\beta\mu_{mc}} \right)^2 \tag{2.13}$$

In the remainder of the text the particle chemical potential ($\beta\mu$) will be referred to as the reduced particle chemical potential, μ^*.

2.3 Results and Discussion

2.3.1 Effects of Polymer Density on Chemical Potential and Polymer Adsorption

Figure 2.1 shows a plot of particle chemical potential (μ^*) vs. polymer density (ρ_p) for different chain lengths at a constant particle size σ_c = 10 and constant colloid-polymer interaction energy $\varepsilon_{cp} = 1 \cdot \varepsilon_{pp}$. It is noted that the confidence intervals have been omitted from all figures unless the error bars were larger than the markers representing simulation results. μ^* decreases with increasing ρ_p and seems to be reaching a minimum value near a polymer density of $\rho_p \approx 0.30$. Computational restrictions have impeded the calculation of μ^* at $\rho_p > 0.20$ and n > 5 and hence the minimum in μ^* is only observed for n = 5. The observed trends are as expected, since increasing the polymer density increases chain adsorption and lowers the particle chemical potential due to the polymer-colloid attractions. However, there is an increase in the excluded volume when polymer density increases, thereby increasing the difficulty of particle insertion. The μ^* trends are determined by competition between these two factors as ρ_p increases, resulting in a minimum value: entropy decreases due to increased excluded volume (more positive μ_c)

and enthalpy decreases due to polymer adsorption (more negative μ_c). We note that a minimum in μ^* with respect to ρ_p is a necessary, although not sufficient, condition for phase instability. The minimum would be followed by a maximum if phase instability were occurring. This may explain the difficulty in achieving equilibration of the simulations in the vicinity of the μ^* minimum.

The effects of adsorption can be further appreciated with Figure 2.2, which shows a plot of absolute adsorption of polymer segments per unit surface area of the particle (Γ_s) vs. polymer density (ρ_p) at $\sigma_c = 10$. As the polymer concentration increases, Γ_s increases because more chains are available to adsorb.

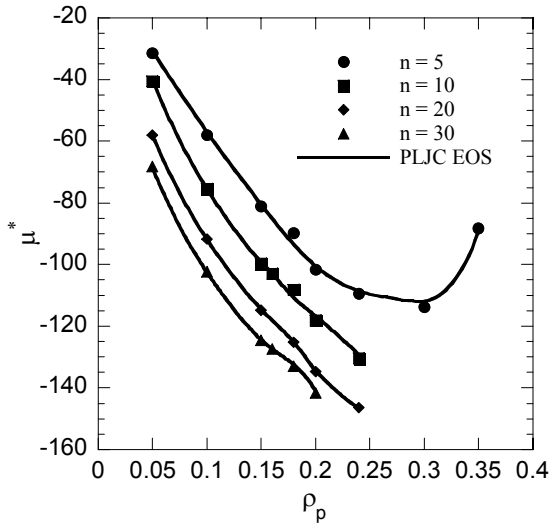

Figure 2.1 - Infinite dilute reduced particle chemical potential ($\mu^* = \beta\mu$) vs. polymer segment density (ρ_p) at different chain lengths (n) for $\sigma_c = 10$. The solid markers (■) represent different values of simulation data and the solid lines (—) represent the PLJC EOS.

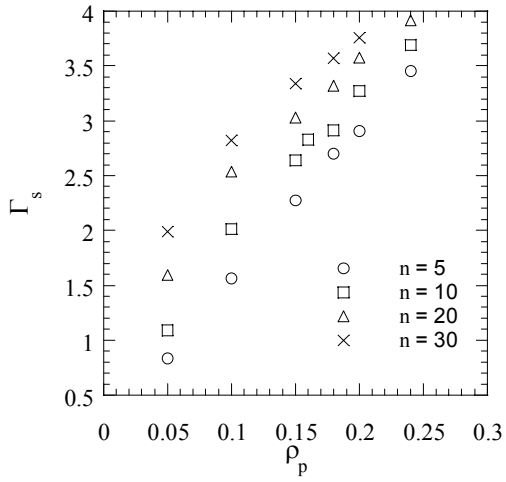

Figure 2.2 - Absolute Adsorption per surface area of the particle (Γ_s) vs. polymer segment density (ρ_p) at different chain lengths (n) for σ_c = 10. The markers represent different values of simulation data.

2.3.2 Effects of Particle Diameter on Chemical Potential and Adsorption

Figure 2.3 shows a plot of μ^* vs. diameter of the colloidal particle (σ_c) at n = 10 and $\varepsilon_{cs} = 1 \cdot \varepsilon_{ss}$ for different values of polymer segment density (ρ_p). μ^* decreases for all values of σ_c at high polymer densities. These results are as expected and follow the same pattern as previously reported[18] for dilute polymer concentrations, due to the dependence of the LJ potential on σ_c. Increasing σ_c increases the range of the LJ potential energy,[18] resulting in a larger number of polymers interacting attractively with the colloidal particle, which in turn decreases the chemical potential. Figure 2.4 illustrates the effects of colloid diameter (σ_c) on excess amount adsorbed (Γ^{ex}) (top) and the excess adsorption per unit surface area (Γ^{ex}_s) (bottom) for different polymer densities. Polymer excess adsorption (Γ^{ex}) increases with σ_c in two distinct ways: (1) in the region $0 < \sigma_c \leq 5$ Γ^{ex} increases slowly with σ_c and (2) for $\sigma_c > 5$, Γ^{ex} increases more rapidly. At lower particle

diameters, the increase in the excess amount adsorbed is mostly due to the increase in the range of the LJ potential energy as previously mentioned. As the particle diameters enters the region where σ_c > 5, another factor in addition to the increase in the LJ potential energy becomes important: surface area of the particle. This is evidenced by the Γ^{ex}_s vs. σ_c plot (Fig. 4 – top) where the amount adsorbed per surface area of the particle (Γ^{ex}_s) is greater at σ_c < 5 leveling out at σ_c > 5 suggesting that the observed adsorption regimes shown in Fig. 4 (bottom) are most likely caused by the greater surface area that allows for more adsorption resulting in the steeper curve at larger particle sizes. This suggests that at the regime where the colloid is small relative to the polymer (σ_c < 5), Γ^{ex} is weakly dependent on ρ_p because there is less surface area for packing of adsorbed chains as compared to σ_c > 5.

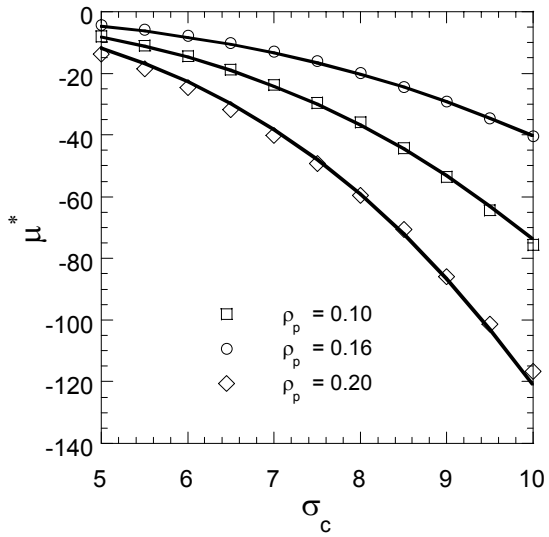

Figure 2.3 - Infinite dilute reduced particle chemical potential ($\mu^* = \beta\mu$) vs. colloid diameter (σ_c) at three different polymer segment densities (ρ_p) for n = 10. The markers represent EEMC simulation data at polymer segment densities of 0.10, 0.16, and 0.20; the solid line (——) represents the PLJC equation of state extended to nanocolloid-polymer mixtures.

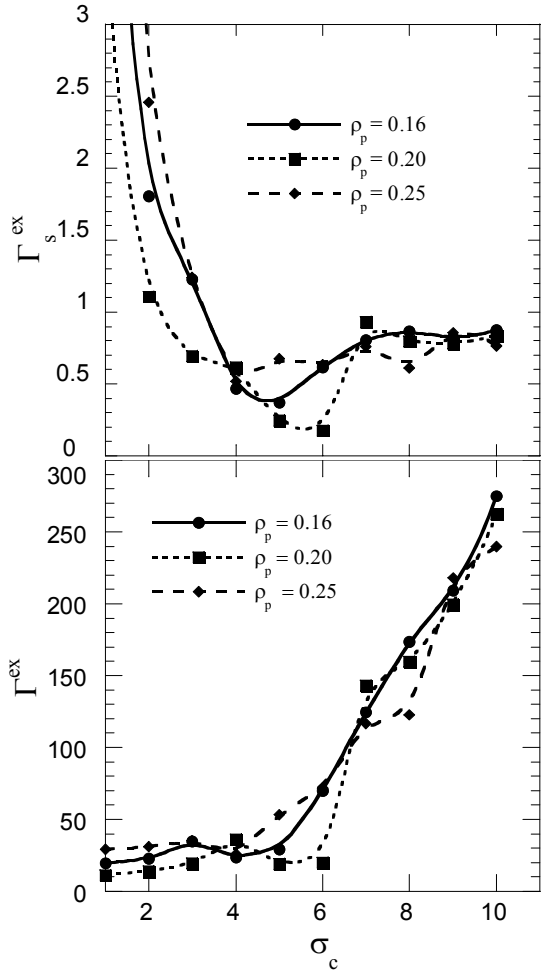

Figure 2.4 - Excess amount adsorbed per unit surface (Γ^{ex}_s) and excess amount adsorbed (Γ^{ex}) vs. colloid diameter (σ_c) at different polymer segment densities (ρ_p) for n = 10. The markers represent different values of simulation data. The lines are a visual aid.

2.3.3 PLJC EOS vs. EEMC Simulation Results - Parameter v_p

The PLJC EOS adapted for nanocolloid-polymer mixtures was tested on the EEMC simulation results at various polymer concentrations *(ρ_p)*, chain lengths *(n)*, and colloid diameter *(σ_c)* in Figures 2.1 and 2.3. The PLJC EOS was able to model the behavior of

colloid-polymer mixtures successfully for all cases with symmetric energy parameters, e.g., $\varepsilon_{sp} = \varepsilon_{pp} = 1$. As in the bulk PLJC for polymer solutions, it was necessary to include the empirical parameter ν_p. In the original PLJC the parameter ν_p ($0 < \nu_p \leq 1$) was used to reduce the large, attractive interaction between the polymer (intersegmental) molecules present in the perturbation term.[1,26] A larger correction corresponds to smaller ν_p values. The variational perturbation neglects intrachain correlations, which become especially important at low ρ_p and low n, where mean-field estimations also fail. So, one expects that in bulk systems the correction will be greater, and hence ν_p smaller, as ρ_p and n decrease. In fact, Chiew et al.[1] and Prausnitz et al.[26] showed that $\nu_p \sim \rho_p$ and $\nu_p \sim n$ for polymer solutions.

Our results for the PLJC applied to colloid-polymer mixtures, show opposite trends in Fig 2.5, where $\nu_p \sim 1/\rho_p$ and $\nu_p \sim 1/n$. Figure 2.5 indicates that ν_p decreases strongly with n^{-y} ($0.8 < y < 1.1$), but is only weakly dependent on ρ_p. Apparently, the molecular reason for the correction is no longer neglect of intrachain interactions, but an attractive contribution that would be over-predicted with *increasing* ρ_p and n. The primary differences between our system and the previously mentioned bulk solutions are (1) chain adsorption on particles and (2) neglect of explicit solvent molecules. As polymer adsorption increases with chain length, a densely-packed layer develops close to the particle surface. The dense layer experiences strong attractions (polymer-polymer and polymer-colloid) that are corrected with lower ν_p values. In fact not only is the dependence of ν_p on n opposite to bulk solutions, but for nanoparticles, the ν_p magnitude ($0 < \nu_p \leq 0.2$) is much less than for polymer solutions ($0 < \nu_p \leq 1$). The absence of explicit solvent can cause an overestimation of the relative contributions of polymer-

polymer interactions to the Helmholtz energy of the system. This fact suggests the need for a net positive correction to account for the "screening" of polymer-polymer interactions that would normally be accomplished with explicit solvent. A similar correction could probably be achieved by adjusting ε_{cp} or T. Regression analysis on Fig 2.5 shows that the empirical ν_p data for different n can be collapsed to one master plot (Fig. 2.6) by plotting $\nu_p \cdot M \cdot n \cdot R_g^x$ vs. ρ_p where R_g is the polymer radius of gyration from EEMC simulations and x = $^5/_3$ is the exponent calculated from the regression analysis. No quantitative molecular significance for the value of x could be drawn, but Figs. 2.5 and 2.6 suggest that ν_p holds qualitative molecular significance. Perhaps this qualitative dependence could be used to motivate predictions of ν_p for other conditions such as larger chain lengths and polymer densities.

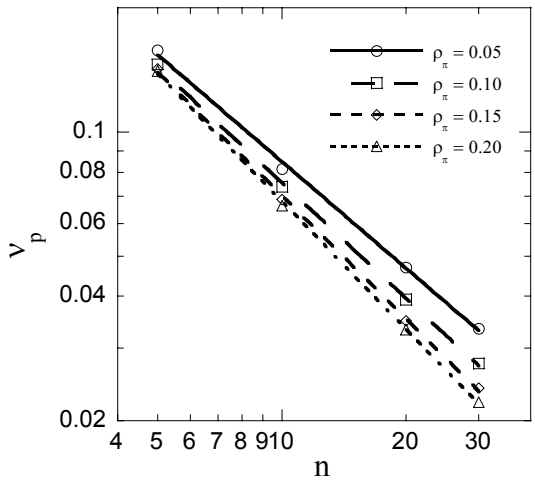

Figure 2.5 – Log-Log plot of the empirical parameter ν_p vs. chain length (n) at different polymer segment densities (ρ_p). The markers represent the ν_p calculated by using the regression procedure outlined previously. The lines are power-law regressions.

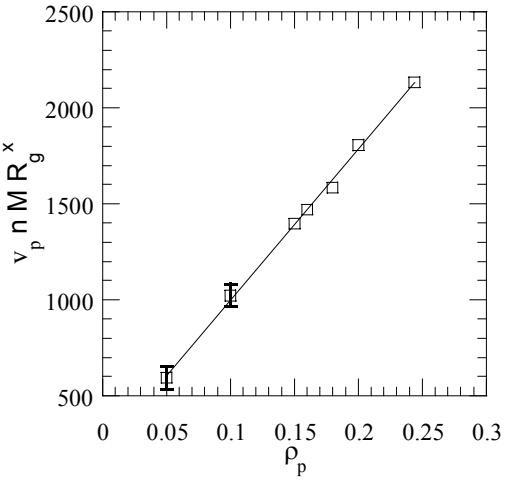

Figure 2.6 - Average ($v_p \cdot R_g^x \cdot m \cdot n$) vs. polymer segment densities (ρ_p) using data for all chain lengths (n). The markers represent averages calculated by using the regression procedure mentioned in Sec. 2.3.3, where $x = {}^5/_3$. The error bars represent 95% confidence intervals. Error bars that were smaller than the markers representing the data have been omitted.

2.3.4 Correction for Adsorption Effects

Figure 2.7 shows that the PLJC EOS extended for nanocolloid-polymer mixtures is unable to predict the behavior of *energetically asymmetric* polymer-colloid mixtures when $\varepsilon_{cp} < \varepsilon_{pp} = 1$. These conditions correspond to the case in which polymer segment-segment attraction is stronger than segment-colloid attraction. At $\varepsilon_{cp} < \varepsilon_{pp} = 1$, the relative importance of polymer-colloid excluded volume increases as compared to polymer-colloid attraction. In a realistic mixture (as in the simulations) the polymer desorbs and eventually becomes depleted from the colloid surface at low ε_{cp}. Depletion is driven by reductions in polymer-colloid excluded volume, making the μ_c relatively less positive. Since the PLJC was not developed to account for polymer adsorption and

desorption on the colloidal particle, the change in polymer-colloid excluded volume is not accounted for properly. While the PLJC can model effectively the symmetric energy case, where adsorption is strong (polymer-colloid attraction dominated), it is missing terms necessary for modeling the complex changes in polymer conformation near the colloid surface when adsorption becomes weak or nonexistent (dominated by repulsive excluded volume interactions). The PLJC thus overpredicts μ^* for weak attraction. The volume that the colloid and polymer segments exclude from one another is approximately proportional to $(\sigma_c^2 \cdot \sigma_p + \sigma_p^2 \cdot \sigma_c)$. We propose a modification term, $\mu^*_{cp} = \beta\mu_{cp}$, to be added to the colloid chemical potential in order to account for these effects.

$$\mu^*_{cp} = C \cdot (\varepsilon_{cp} - \varepsilon_{pp})(\sigma_c^2 \cdot \sigma_p + \sigma_p^2 \cdot \sigma_c) \tag{2.14}$$

Eq. (2.14) is a simple semi-empirical correction that "turns on" linearly as ε_{cp} becomes different from ε_{pp}. The constant C is determined via least-squares regression to obtain a fit to the experimental data, as indicated in Figure 2.7, resulting in values close to 0.108 in all cases explored. The modified PLJC, mPLJC, is obtained by adding μ^*_{cp} to the μ^* obtained in eq. (2.11). Table 2.2 shows the correction (μ^*_{cp}) and the corrected chemical potential (μ^*) and C for all values of ε_{cp} and σ_c explored here. The solid lines in Figure 2.7 show that the correction allows nearly perfect agreement between theory and simulation.

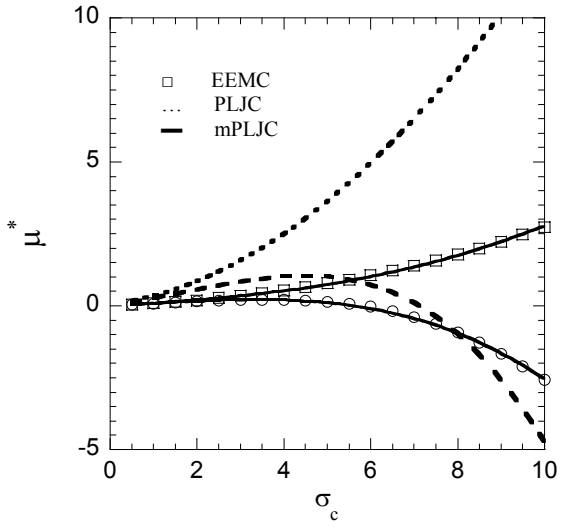

Figure 2.7 - Infinite dilution colloid chemical potential (μ^*) vs. colloid diameter (σ_c) at different interaction energies (ε_{cp}) for n = 10. The markers represent EEMC simulation data at ε_{cp} of 0.05 and 0.25, where the square markers (□) represent ε_{cp} = 0.05 and the circular markers (○) represent ε_{cp} = 0.25. The solid lines (**—**) represent the mPLJC equation of state with the inclusion of the correction term, and the dotted lines represent the PLJC without the correction (····) for ε_{cp} = 0.05 and (- - -) for ε_{cp} = 0.25.

Table 2.2 – Corrected reduced chemical potential (μ^*), adsorption correction (μ^*_{cp}), and the constant C for different values of ε_{cp} and σ_c studied.

	ε_{cp} = 0.5		ε_{cp} = 0.25		ε_{cp} = 0.05		ε_{cp} = 0.005	
	C = 0.1078		**C** = 0.1083		**C** = 0.1080		**C** = 0.1081	
σ_c	μ^*	μ^*_{cp}	μ^*	μ^*_{cp}	μ^*	μ^*_{cp}	μ^*	μ^*_{cp}
1	0.079	0.108	0.087	0.162	0.097	0.205	0.108	0.215
2	0.104	0.324	0.169	0.486	0.205	0.616	0.211	0.645
3	-0.010	0.648	0.218	0.972	0.344	1.231	0.341	1.290
4	-0.343	1.080	0.210	1.620	0.519	2.052	0.506	2.149
5	-0.977	1.620	0.116	2.430	0.740	3.078	0.715	3.224
6	-1.993	2.268	-0.088	3.402	1.014	4.309	0.974	4.513
7	-3.473	3.024	-0.430	4.536	1.347	5.746	1.291	6.018
8	-5.497	3.888	-0.936	5.832	1.749	7.387	1.675	7.737
9	-8.148	4.860	-1.632	7.290	2.225	9.234	2.133	9.671
10	-1.508	5.940	-2.547	8.910	2.784	11.286	2.672	11.821

2.3.5 Fit to Experimental Data

Recently, a new technique that allows for direct measurement of particle chemical potential (μ_c) from membrane osmometry was demonstrated.[37] This previous experimental study investigated the effects of polymer and colloid concentration on μ_c of nanocolloidal silica (diameter dispersion = 10-20 nm) in a poly(ethylene oxide) (PEO) (molecular mass = 2000) aqueous solution. To see if the experimental data could be reproduced by the mPLJC, the regression procedure described below was used. To our knowledge, no LJ parameters for the silica-PEO-water system are available in literature. Thus, we found it necessary to introduce an additional empirical parameter (f) to mimic the relative contribution of the interaction energies, thus $\varepsilon_{pp} = f \cdot \varepsilon_{cc}$. The mPLJC effective chain length was calculated by using the concept of an equivalent freely jointed chain.[18,60] Accordingly, $\check{n}l^2 = R^2_{eed}$ and $(\check{n}l)^2 = l_f^2$ and $\check{n} \approx l_f^2/R^2_{eed}$ where $\check{n}$ is the length of an equivalent Gaussian chain, l_f is the fully extended chain length, l is the segment length, and R_{eed} is the polymer end to end distance. A persistence length (l_p)[60] is used to correlate between real segment length and the polymer model segment length. Then $\check{n} \approx M_{avg} / l_p \cdot M_{monomer}$ and for the PEO molecular mass used in the above mentioned experiment, the effective chain length for the mPLJC is $\check{n} \approx 13$. The number of chains was calculated by matching the polymer segment volume fraction and experimental polymer volume fraction. The PEO monomer length has been reported as $l \approx 4\text{Å}$;[61-63] therefore a colloid to polymer segment size ratio of $\sigma_{colloid}/\sigma_{polymer} \approx 25$ was used in the mPLJC. The experimentally observed trends are compared to the mPLJC equation in Fig 2.8. Satisfactory agreement between calculated and experimental μ_c were obtained at the higher PEO concentrations. Deviations occurred at lower PEO concentrations. The

deviations are due most likely to the dependence of v_p and C on SiO_2 concentration (C_{si}) because we have treated v_p and C to be independent of C_{si}. We believe there is still room for improvement in the mPLJC predictions for nanoparticles-polymer systems and a better fit could be obtained with further investigation of C_{si} sensitivity on the empirical parameters. The least-square regression results are shown in Table 2.3. The empirical parameter f did not vary considerably with different PEO concentrations and therefore $\varepsilon_{pp} \approx 3.2 \cdot \varepsilon_{ss}$. Although the fitting shows the mPLJC EOS can account for the experimental observations, the regression is somewhat arbitrary due to the large number of adjustable parameters. It is noted that only error bars for 5 mass % PEO from an osmometer validation study[37] are shown.

Table 2.3 – Result of the mPLJC empirical parameters calculated from the regression analyses between EOS prediction and membrane osmometry experiments.

	7 mass % PEO	5 mass % PEO	2 mass % PEO
v_p	0.0117	0.0149	0.0282
C	0.0426	0.0855	0.1239
f	3.221	3.201	3.213
M	612	427	166

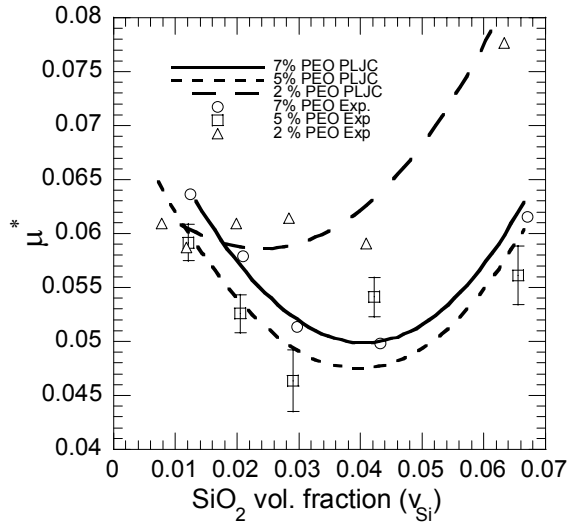

Figure 2.8 – Reduced colloid chemical potential ($\mu^*=\mu/kT$ (PLJC) or $\mu^*=\mu M_w/RT$ *(experiment))* vs. silica volume fraction (v_{si}) at different PEO mass %. The markers represent membrane osmometry data, where the triangular markers (Δ) represent PEO mass % = 2, the square markers (□) represent PEO mass % = 5, and the circular markers (○) represent PEO mass % = 7. The solid line (—) represents the mPLJC equation of state for 7 mass % PEO , and the dotted lines represent the mPLJC (····) for 5 mass % PEO and (- - -) 2 mass % PEO. The error bars shown are 95% confidence intervals.

2.4 Conclusions

The EEMC method was extended to semi-dilute polymer concentrations for a nanocolloid in a freely adsorbing polymer solution. Simulation results were used to validate the predictions of the PLJC equation of state extended to model these polymer-nanocolloid dispersions. The effects of the polymer segment density (ρ_p) on the particle chemical potential (μ_c) and polymer adsorption (Γ) were investigated. In general, μ_c decreases with increasing ρ_p, approaching a minimum, while Γ increases with ρ_p. These trends are due to competition between the enthalpy (attractive) and entropic (repulsive) effects of polymer adsorption. The PLJC EOS showed very good agreement with EEMC

simulation results for all n, ρ_p, and σ_c with energetic symmetry. The empirical parameter (ν_p), introduced by others to adjust the overly attractive perturbation, was necessary to obtain agreement between theory and simulation. Our regression analyses performed indicates that $\nu_p \sim R_g^{3/5}$. Furthermore, the collapse of ν_p values into one master plot shows that ν_p could be predicted without having to regress additional simulation data.

The PLJC EOS did not predict accurately the simulation data for energetic asymmetric cases, e.g., $\varepsilon_{cs} < \varepsilon_{pp}$. This shortcoming is most likely due to the μ^* dependence on polymer-colloid excluded volume when the strength of attraction is diminished. We propose a semi-empirical modification term that corrects for polymer-colloid excluded volume when adsorption of polymer is weak. The modified PLJC, mPLJC, was able to predict satisfactorily the simulations for energetic asymmetry. Finally, we fitted the mPLJC model to μ^* values from membrane osmometry[37] experiments for PEO-silica dispersions. Deviations from experiment are most likely due to ν_p dependence on C_{si}.

We conclude that polymer adsorption dominates the chemical potential, which can be of great importance in the study of how adsorbed polymer layers affect nanocolloid stability and phase behavior. Accurate equations of state for nanocolloid-polymer mixtures must account for the effects of adsorption on polymer conformations. These EOS can be used describe how the addition of adsorbing polymers will affect thermodynamic behavior, and are essential to the future of advanced nanomaterial fabrication and chemical processing.

CHAPTER III

MEASUREMENT OF ORGANICALLY-MODIFIED NANOPARTICLE CHEMICAL POTENTIALS USING OSMOMETRY

The potential applications of dispersed and self-assembled nanoparticles depend critically on accurate control and prediction of their phase behavior. Often, polymer or oligomer additives are used to modify the dispersability and self-assembly conditions, although no predictive models exist for design of organic modifiers. The chemical potential (μ) is essential in describing the equilibrium distribution of all components in each phase, is a sensitive indicator of local molecular environment, and is defined rigorously in classical and statistical thermodynamics. This chapter presents a unique application of osmotic pressure measurements for the calculation of μ of nanocolloidal silica in an aqueous solution of adsorbing poly(ethylene oxide) (PEO). The trends from experiments agreed well with Monte Carlo simulations for the dependence of chemical potential on concentrations and temperature. Polymer adsorption was found to be the most influential variable, determining the balance between attraction and repulsion that ultimately leads to μ decreasing (attractive) or increasing (repulsive) with polymer concentration.

3.1 Introduction

In recent years, there has been considerable interest in nanoscale materials fabrication, due to the unique optical, electronic, mechanical, and chemical properties that depend sensitively on particle size. Nanostructured materials promise novel applications in practically all fields of science, engineering, and medicine. However, one of the grand challenges facing nanotechnology is the large-scale manufacturing of devices in a controlled, predictable, and repeatable manner. Colloidal nanoparticles, "nanocolloids", are one of the most commonly utilized systems for assembly of ordered nanostructures. As most nanoparticles are unstable in solvent dispersions, polymers and oligomers are used widely as stabilizing agents to prevent uncontrolled flocculation and promote organized self-assembly[2]. Organic modifiers are also used to passivate and "cap" reactive groups on nanoparticle surfaces. It is well-known that variations in polymer chain length, adsorption, and chemistry can be used to adjust the stability of colloidal dispersions.[36] Few experiments, however, report controlled studies of nanoparticle stability as a function of modifier properties, or measurements of fundamental thermodynamic quantities. In addition, a lack of robust models for design of organic modifiers and the interpretation of experiments makes nanofabrication process-design a distant challenge. Some examples of organically-modified nanocolloidal systems include self-assembled silica grafted with polystyrene-poly(benzyl acrylate) block copolymer,[4] multidimensional structures of metal nanocrystals with alkane thiols,[5,6] Pd nanoparticles stabilized with poly(vinylpyrrolidone),[7] and gold nanocrystals stabilized using dodecanethiol.[64,65]

Theoretical[9-14] and simulation[16,17] efforts have aimed to develop molecular-based approaches for describing the phase behavior of colloid-polymer systems. Most efforts have focused on hard-sphere, repulsive models that do not account for particle-polymer attraction that occurs in organically-modified systems. Recently, expanded ensemble Monte Carlo (EEMC) simulation[38,40,41] was adapted to calculate chemical potentials of organically-modified nanoparticles using hard-sphere[42] and attractive Lennard-Jones (LJ) models.[18] These simulations indicated the sensitivity of the particle chemical potential, μ_c, to the local molecular environment and particularly to polymer adsorption in attractive systems. Since μ_c is defined rigorously in thermodynamics, phase behavior and equations of state can be calculated if appropriate μ_c models can be developed. An experimental method for measuring μ_c in attractive nanoparticle-polymer systems would be an important advance towards these goals.

Experimental studies in attractive systems composed of polymer (or surfactant) and particles have demonstrated the effects of modifier adsorption on nanoparticles,[30,31] including the PEO-silica system.[32-35] These studies have focused on phenomena that depend indirectly on polymer and particle chemical potentials, such as phase behavior, osmotic compressibility, and polymer adsorption. To our knowledge, no direct measurements of μ_c have been reported. This chapter describes the use of membrane osmometry to measure μ_c in a model organically-modified system: silica nanoparticles in a poly-ethylene-oxide (PEO) aqueous solution. The results are compared to EEMC simulations of an analogous LJ nanoparticle – adsorbing polymer system.

3.2 Theory

3.2.1 Osmotic Pressure and Chemical Potential

In this study, we are interested in investigating the effects of temperature and polymer and colloid concentration on nanoparticle μ_c. Extensive thermodynamic descriptions of osmometry measurements have been published,[66-70] thus only a brief development is given below. Osmotic pressure is the pressure needed to stop the influx of solvent through a semi-permeable membrane (permeable only to solvent, not solute) separating pure solvent from solution. Fig 3.1 shows a schematic diagram of the osmometer adapted to our three-component system, with solvent and modifying polymer in equilibrium between phases α and β, but with the nanocolloid only in phase β.

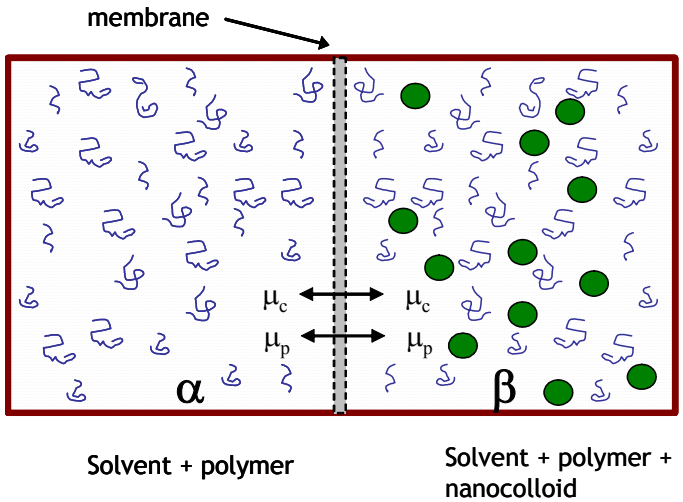

Figure 3.1 - A schematic diagram of the three-component system in this study. The ● represents the nanocolloid, ⌇ represents the polymer.

The equation of chemical potential equilibrium for component *i* between phases α and β is:[69]

$$\mu_i^{\alpha} = \mu_i^{\beta} \tag{3.1}$$

The fundamental energy balance on phase β is:[69]

$$dU = TdS - PdV + \sum_i \mu_i dn_i \tag{3.2}$$

where the subscript *i* denotes species, *S* is the total entropy, *V* is the total volume, *T* is the temperature, *P* is the total pressure, *U* is internal energy, and n_i is the mole number. Application of Euler's theorem to eq. (3.2) followed by differentiation gives:

$$dU = TdS + SdT - PdV - VdP + \sum_i \mu_i dn_i + \sum_i n_i d\mu_i \tag{3.3}$$

Comparing eq. (3.2) and eq. (3.3) yields the Gibbs-Duhem equation:[69]

$$SdT - VdP + \sum_i n_i d\mu_i = 0 \tag{3.4}$$

The Gibbs-Duhem equation is then used to describe the relationship between osmotic pressure and chemical potential. Since both phases of our system are held at identical constant temperature, $dT = 0$, and the volume is constant, eq. (3.4) can be reduced to the following:

$$-VdP + n_s d\mu_s + n_p d\mu_p + n_c d\mu_c = 0 \tag{3.5}$$

where subscripts *s, p,* and *c* denotes the solvent, polymer, and nanoparticle, respectively. At equilibrium there is no change in the solvent ($d\mu_s = 0$) or polymer ($d\mu_p = 0$) chemical potential; therefore, eq. (3.5) can be further simplified to:

$$VdP = n_c d\mu_c \tag{3.6}$$

Integration of eq. (3.6) at constant n_c, with a lower limit of integration P_0, μ_{c0} for a system of solvent and polymer only ($\mu_{c0} = 0$) and an upper limit of P, μ_c for a system of solvent, polymer, and particle gives:

$$V\pi = n_c \mu_c \tag{3.7}$$

where π is the osmotic pressure ($P_1 - P_0$), and μ_c is the nanoparticle chemical potential. Converting molar to mass concentration, we arrive at

$$\mu_c = \frac{\pi}{C_c} \tag{3.8}$$

where C_c is the concentration of solute in kg/m^3, and π is the osmotic pressure in Pa. Both eqs. (3.7) and (3.8) satisfy the Gibbs-Duhem thermodynamic relationship for osmotic pressure:[70] $(\partial\pi / \partial n_c)_{T,\mu S} = n_c\ (\partial\mu_C / \partial n_c)_{T,\mu S}$. For the remainder of this chapter, we use the dimensionless reduced chemical potential (μ^*) where $\mu^* = \mu_c \cdot M_w / RT$ (M_w is the molar mass of SiO_2) for the experimental results and $\mu^* = \mu_c / kT$ for the EEMC simulation results.

3.2.2 Chemical Potentials from Expanded Ensemble Monte Carlo Simulation

In this study previously published[18] and new results[71] from Expanded Ensemble Monte Carlo (EEMC) simulations are used to interpret the molecular significance of the osmotic pressure experiments. The simulation system consisted of nanoparticles dispersed in a solution of freely-adsorbing polymer chains with Lennard-Jones (LJ) interactions. Experimental studies[30-32,72] suggest that the PEO-silica nanoparticle system resembles the simulation model system,[18,71] in that PEO has strong attractive interactions with silica and adsorbs. A brief description of the EEMC model system is given here, with details given elsewhere.[18,71] Polymer chains are freely-jointed tangential LJ spherical segments with constant bond length, σ_p. The nanoparticle is modeled as a LJ sphere with diameter σ_c. The solvent molecules are not accounted explicitly in the simulation, but variations in the reduced temperature (T^*) mimic changes in relative magnitudes of attractive and repulsive interactions and solvent "quality". At best, the use of a LJ potential to model polymer segment – nanoparticle interactions is a gross oversimplification. A better approximation would be an integrated LJ interaction between a polymer segment and all LJ atoms in the nanoparticle. In this case, the exponents and coefficients change, but the fundamental form of the inverse power law function is preserved. One of the features of all inverse power law functions, regardless of the coefficients and exponents, is that the range of the potential scales linearly with nanoparticle diameter. Although magnitudes may not be modeled well here, the essential feature is preserved: the range of nanoparticle van der Waals interactions increases as more atoms are added to the nanoparticle. We suggest that although the EEMC model is

an idealized system, it can be used as a basis for understanding the fundamental driving forces of the observed phenomena.

3.3 Experimental Section

3.3.1 Materials and Sample Preparation

Poly-dispersed PEO of relative molecular mass M_r = 2000 was purchased from Fluka Chemika. SNOWTEX-40® aqueous nanoparticulate silica dispersion was purchased from Nissan Chemical Industries, Ltd. SNOWTEX® is stabilized by the negatively-charged surface chemistry of the amorphous silica nanoparticles. The composition was 40 mass % SiO_2, less than 0.6 mass % Na_2O, and the balance water. The spherical silica nanoparticles have a particle diameter range of 10-20 nm as reported by the manufacturer. De-ionized (DI) water was used to prepare samples containing various combinations of silica and PEO by mixing with a magnetic stirrer for twenty minutes or until all components dissolved. The composition of the samples had a range of 2-15 mass % silica and 2-10 mass % PEO. Cellulose Acetate membranes with a 20,000 Dalton cutoff were purchased (Universal Instrument Company (UIC) Inc) and conditioned by immersing in DI water / iso-propanol mixtures for a period of 8 hrs with frequent stirring to remove any process contamination. The membrane was then placed in pure DI water for a minimum of 6 hrs. The study was performed at three different temperatures, T = 298 K, 309 K, 314 K.

3.3.2 Experimental Apparatus and Methodology

A model 231 Recording Membrane Osmometer (UIC Inc.) was used to record osmotic pressure. The osmometer consists of a single cell divided by the semi-permeable membrane into two compartments of 0.15 mL (the solution chamber β and the solvent chamber α). The cell membrane is held rigidly between the two compartments completely separating them; no liquid can pass from one compartment to the next without either going through the membrane or through the valve system controlling filling or draining. The solvent chamber was always filled with either pure DI water or DI water – PEO solution. When a solution containing silica particles is placed in the solution chamber, differences in solvent and polymer chemical potential between both compartments causes the solvent and polymer to diffuse through the membrane into the solution compartment. A steel diaphragm on one end of the solvent chamber is connected to a transducer that monitors pressure changes caused by the loss of solvent and polymer. The pressure reduction is the osmotic pressure, π. Any future reference to solvent refers to the water-PEO mixture and the solvent-polymer-particle mixture is referred to as the solution.

A reference pressure reading with solvent in both compartments was made first, followed by measuring the solution osmotic pressure by subtracting the solution pressure reading from the reference pressure. In this manner, the reference state is the polymer-water system with no nanoparticle added, e.g., nanoparticle is isolated from the solvent, and is the same as the "vacuum" reference in the EEMC simulations. Each pressure measurement was taken in triplicate to provide for statistical analysis and to assure that the system had reached thermal equilibrium. The samples were organized and tested in

runs of varying silica concentration at constant PEO concentration, beginning with the lowest silica concentration. Multiple runs at 5 mass % PEO using the same sample were made to investigate the precision of the osmometer measurements. The results are shown in Fig 3.2. Several validation studies were performed to corroborate that the membrane is permeable to PEO of M_r = 2000, but not to silica particles. Osmotic pressure measurements between samples of pure DI water and a 2 mass % PEO solution showed an exponential decrease approaching half of the initial π reading in 1 h, which remained constant without any fluctuations for the duration of the experiment (1 h). This suggests that the PEO was diffusing through the membrane until the PEO concentrations in both chambers were equal (chemical equilibrium). Another 2 mass % PEO solution was immediately tested without draining the solvent chamber, and the same behavior was observed. The osmotic pressure recorded was halfway between that of the newest 2 mass % solution and the equilibrium value from the previous validation experiment. The same procedure was followed for samples of pure DI water and a 2 mass % silica solution. The osmotic pressure *did not fluctuate* and remained *constant* for the entire duration of the experiment (2 h). This result demonstrated that the silica particles do not diffuse through the membrane and the membrane is therefore permeable only to PEO. The osmometer was used to measure the molecular mass of poly(vinyl acetate) (PVA) (VWR) to within 10% of the manufacturer's reported average molecular mass of 75,000.

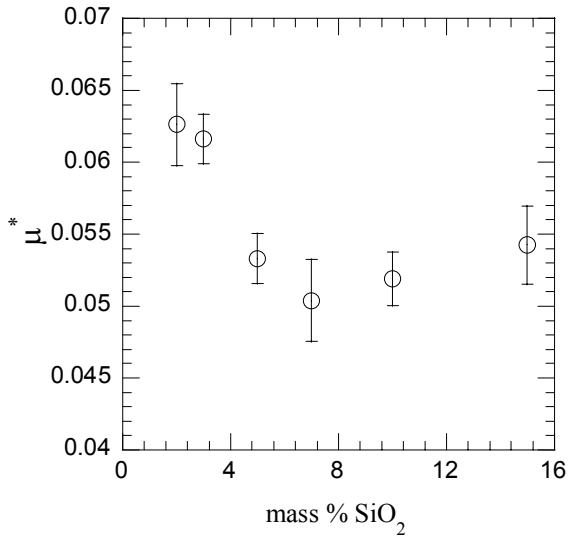

Figure 3.2 - Reduced particle chemical potential ($\mu^* = \mu \cdot M_w$ /RT) as a function of silica mass % for 5 mass % PEO. The markers denote the average value of multiple experimental runs under constant conditions and the error bars shown are 95% confidence intervals.

3.4 Results and Discussion

3.4.1 Effects of Silica Concentration

In order to interpret the data from the osmotic pressure measurements as a function of silica concentration the reduced particle chemical potential (μ^*) is plotted vs. silica volume fraction (v_{si}) for different PEO mass percentages (x_{PEO}) as shown in Fig 3.3. Note that confidence intervals have been omitted from all figures unless the error bars were larger than the markers representing the data. Table 3.1 shows the osmotic pressure measurements for the different PEO and silica mass percentages. As shown in Fig 3.3, in the pure silica-water system (0 mass % PEO), μ^* increases with v_{si} indicating a positive increase in the free energy of the system as more silica is added. The trend resembles a system dominated by repulsive excluded volume interactions, and agrees qualitatively

with EEMC simulation results, shown in Fig 3.4. For $x_{PEO} > 0$, the nanoparticle chemical potential decreases as silica concentration increases up to a minimum at which the trend reverses and the chemical potential increases. The experimental (Fig 3.3) and computer simulation trends[18] (Fig 3.4) agree qualitatively in these cases also, in that the minimum in μ^* with v_{si} is seen only when adsorbing PEO is present in the system. In the simulations, it was observed that the minimum μ^* was due to competition between polymer adsorption (more attraction and negative μ^*) and the increased excluded volume (repulsion between polymer and particle) as v_{si} increases.[18] The experiments showed displacement of the μ^* minimum to higher v_{si} as PEO concentration increased. One possibility is that at higher polymer concentrations more surface area (more particles) will be needed for the adsorbed polymers to reach surface saturation. Once saturated, the excluded volume effects may take over, giving rise to the shift in minimum to higher v_{si} to give an optimum surface coverage. In the simulations the position of the minimum does not move to higher v_{si} as polymer concentration, probably because the simulations were performed at $\sigma_c = 5 \cdot \sigma_p$ where the adsorption energies are relatively weak (because of the size of the colloidal particle) as compared to the experiments where polymer adsorption was a dominating factor in determining the μ_c trends.

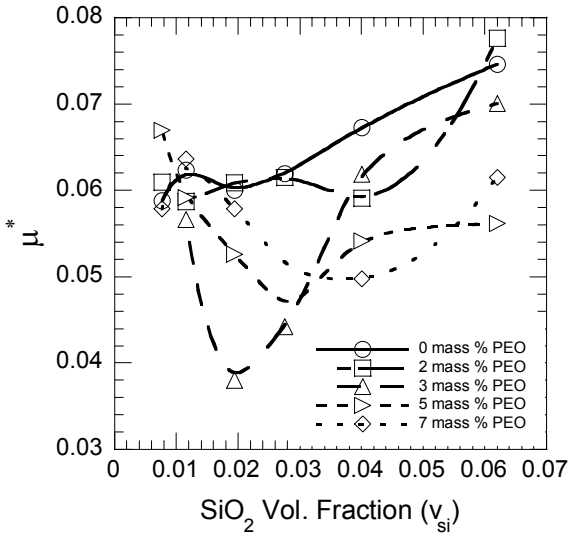

Figure 3.3 - Reduced particle chemical potential ($\mu^* = \mu \cdot M_w / RT$) as a function of silica volume fraction (v_{si}) for different PEO mass %. The markers denote the actual osmometric measurements and the dotted lines are used merely as a visual aid.

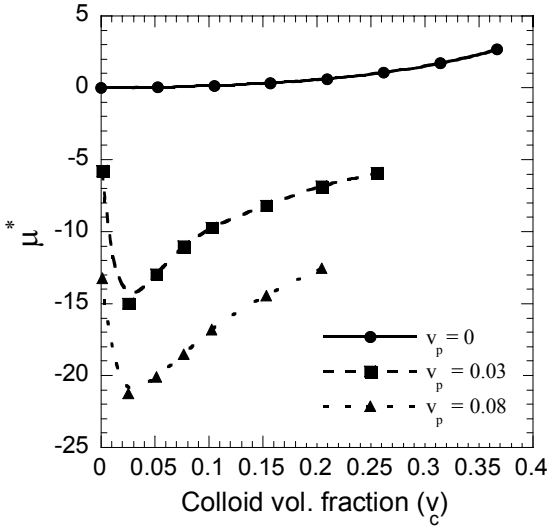

Figure 3.4 - EEMC simulation reduced particle chemical potential ($\mu^* = \mu/kT$) as a function of colloid volume fraction (v_c) for different polymer volume fractions (v_p). The colloids have a diameter $\sigma_c = 5\ \sigma_p$, where σ_p is the diameter of a polymer chain segment and the polymer chain length (n) = 30. The markers denote the actual EEMC simulation results, the lines are used merely as a visual aid.

3.4.2 Effects of poly(ethylene oxide) Concentration

The reduced particle chemical potential (μ^*) is plotted vs. PEO volume fraction (v_{PEO}) for different mass % silica in Fig 3.5. As PEO is added to the system, μ^* decreases until a minimum point where μ^* increases again with v_{PEO}, similar to the dependence on $v_{Si.}$ The particle chemical potential decreases initially with addition of polymer, most likely due to adsorption of PEO on silica. Adsorption of PEO on silica has been observed experimentally using photon correlation spectroscopy (PCS),[72] nuclear magnetic resonance solvent relaxation (NMR),[32,73] and small-angle neutron scattering (SANS).[31] Fig 3.6 shows results from the EEMC simulation study of freely adsorbing polymer chains on a nanocolloid, which show a decrease in particle chemical potential with increasing polymer concentration, directly correlated with increased adsorption.[71] No minimum in the chemical potential trend is observed at high polymer concentration in the EEMC simulation results which may be due to the large free volume available for polymer addition in the infinitely-dilute nanoparticle simulation. The simulation trends demonstrate qualitatively that a decrease in particle chemical potential is caused by an increase in polymer adsorption arising from higher polymer concentration.[71] At high polymer concentration the experimental nanoparticles experience increased repulsive excluded volume interactions due to the decrease in available free volume for the particles. Particles likely become saturated with polymer near the minimum as shown in Fig 3.5. One can see that in the simulation results in Fig 3.6, the slope of μ^* vs. v_p appears to be approaching zero, although computational restrictions at high polymer concentration have prevented the observation of a minimum. In addition, it must be remembered that the simulations results in Fig 3.6 neglect particle-particle interactions.

Osmotic μ measurements can indicate where phase instability points occur and future work is planned to pursue this goal. The appearance of minima in the nanoparticle μ^* as a function of x_{PEO} signifies a necessary, although not sufficient, condition for phase instability, since minima in μ^* are equivalent to inflection points in the mixture free energy.[69] The inflection point (μ^* minimum) must occur at an x_{PEO} that is between two local minima in the mixture free energy in order for instability and separation into two equilibrium phases to occur. A free energy curve with two local minima (separated by a maximum) would be indicated by a nanoparticle μ^* vs. x_{PEO} plot with a minimum followed by a maximum as x_{PEO} is increased.[69] The dependence of μ^* on x_{PEO} seen in Figs 3.5 and 3.6 shows a minimum first, but a maximum was not observed over the range of compositions explored. The same analysis applies to the μ^* vs. x_{Si} plots (Figs. 3.3 and 3.4), except that the order of the minimum and maximum is reversed. As x_{Si} (nanoparticle) is increased, a maximum in μ^* followed by a minimum is necessary and sufficient evidence for phase instability. As Figs. 3.3 and 3.4 show, the minimum in μ^* occurs first, and no maximum is observed. Therefore, the value of x_{Si} at the μ^* minimum in Fig 3.3 cannot be an instability point, as it cannot lie between two free energy minima (for two equilibrium phases).

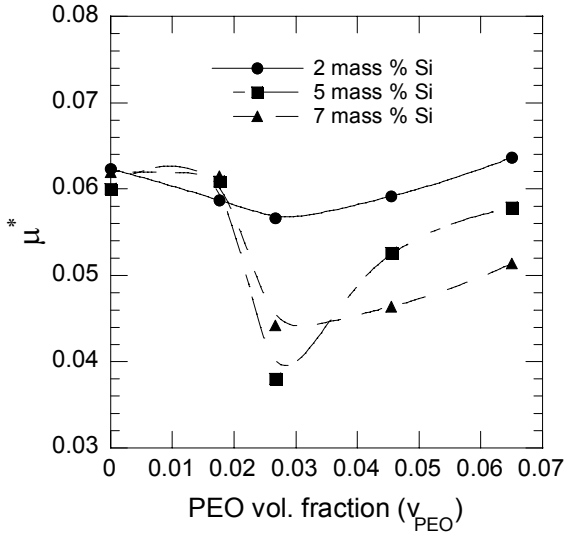

Figure 3.5 - Reduced particle chemical potential ($\mu^* = \mu \cdot M_w / RT$) as a function PEO volume fraction (v_{PEO}) for different mass % SiO_2. The markers denote the actual osmometry measurements and the lines are used merely as a visual aid.

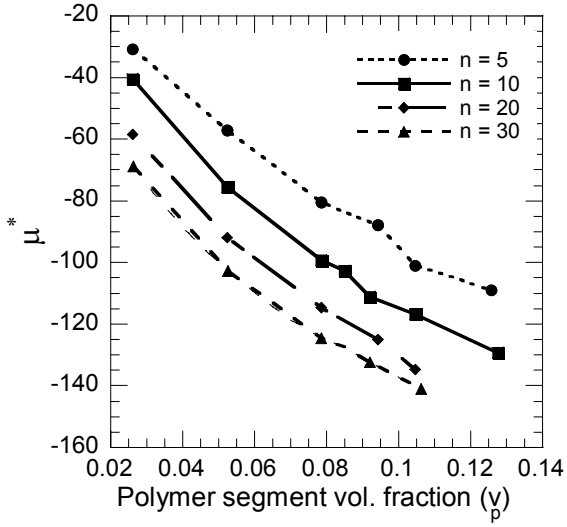

Figure 3.6 - EEMC simulation reduced particle chemical potential ($\mu^* = \mu/kT$) as a function of polymer segment volume fraction (v_p) for different chain lengths (n). The markers denote the actual simulation results, the lines are used merely as a visual aid.

Table 3.1 – Osmotic pressure results for different PEO concentrations and at different temperatures.

T = 298 K

PEO = 0 mass %		PEO = 5 mass %		PEO = 7 mass %	
Mass % SiO_2	Π (Pa)	Mass % SiO_2	Π (Pa)	Mass % SiO_2	Π (Pa)
2	49.0	2	58.8	2	52.0
3	78.5	3	78.5	3	86.3
5	127.5	5	117.7	5	132.4
7	186.3	7	147.1	7	166.7
10	294.2	10	250.1	10	235.4
15	505.0	15	402.1	15	451.1

PEO = 5 mass %

T = 298 K		T = 309 K		T = 314 K	
Mass % SiO_2	Π (Pa)	Mass % SiO_2	Π (Pa)	Mass % SiO_2	Π (Pa)
2	58.8	2	81.7	2	98.1
3	78.5	3	114.4	3	147.1
5	117.7	5	179.8	5	228.8
7	147.1	7	248.4	7	353.0
10	250.1	10	474.0	10	670.1
15	402.1	15	800.9	15	1487.3

3.4.3 Effects of Temperature

The effect of temperature (T) on the particle chemical potential was also investigated. Fig 3.7 shows that the reduced particle chemical potential, μ^*, increases with increasing T. The trends suggest that the attractive interaction and adsorption of polymer on the nanoparticles is greatest at the lower temperature. EEMC simulations (not shown) also show an increase in μ^* when increasing T^*, caused by the decrease in polymer adsorption.[18,71] Fig 3.7 suggests that the highest T (314 K) comes close to the behavior of the repulsive silica-water system (no PEO) with only repulsive excluded volume interactions, shown in Fig 3.4.

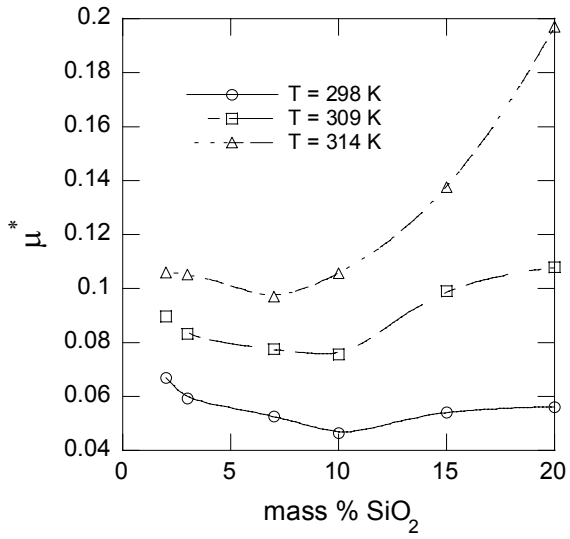

Figure 3.7 - Reduced particle chemical potential ($\mu^* = \mu \cdot M_w / RT$) as a function of mass % SiO_2 at different temperatures for 5 mass % PEO. The markers denote the actual osmometric measurements and the lines are used merely as a visual aid.

3.5 Conclusions

Nanoparticle chemical potentials calculated from osmotic pressure were reported for an aqueous PEO-silica system in the range of 298-314 K. The osmometry method of measuring nanoparticle properties has the potential to become a standard technique for characterization and design of organic nanoparticle modifiers. The method is attractive because it provides insight into the molecular environment of nanoparticle mixtures and dispersions through a relatively facile experiment. Such insight is critical to support ongoing simulation and theoretical efforts to develop accurate equations of state and phase behavior predictions.

In the PEO-silica system, the nanoparticle μ^* decreases, passes through a minimum, and increases again as PEO or silica concentration increase. This trend agrees qualitatively very well with published EEMC simulation results. In the simulations, which neglect nanoparticle-nanoparticle interactions, the minimum in μ^* with polymer concentration was not observed. The effect of temperature on chemical potential also agrees well with EEMC simulation results.

The simulations indicate that the minimum in μ^* versus v_{PEO} or v_{si} is due to competition between entropy (due to repulsive excluded volume interactions at high concentrations) and enthalpy (due to attractive interactions and adsorption of polymer). This suggests the existence of an optimum polymer concentration for the minimization of the free energy of dispersion. This concept could lead eventually to a design rule for nanoparticle stabilizers.

CHAPTER IV

CONCLUSIONS

Nanoparticle chemical potentials were calculated for attractive nanocolloid-polymer systems from EEMC simulations and compared to experimental values measured with osmometry. In addition, an EOS that has been adapted from a perturbed polymer chain EOS has been proposed and reproduces the simulation results exceptionally well. The modified PLJC EOS can serve as a basis from which more accurate chemical potential models can be constructed; these can be used to predict phase behavior and stability. The osmometry method for measuring nanoparticle chemical potentials has the potential to become a standard technique for characterization and design of organic modifiers for nanoparticles. In addition, the EEMC simulations adapted beyond the dilute polymer concentration regime provided molecular insight into the dependence of nanoparticles chemical potential on polymer concentration, colloid size, and adsorption.

One of the major obstacles in designing nanoparticle modifiers is that little is known on how the physical and chemical characteristics of the modifier affect phase stability. The experimental and simulation knowledge gained from this study can be used as a basis to guide further research focused in understanding nanoparticle-modifier phase stability and developing more accurate thermodynamic models. Furthermore, the

understanding gained can lead to concepts such as the existence of optimum polymer concentration, chain length, or temperature for the minimization of the free energy of a nanoparticle-polymer dispersion that could guide eventually to design rules for nanoparticle stabilizers. In addition, osmometry can become a standard method for testing these thermodynamic models. By understanding how surface modifiers affect phase stability, one could design and produce customized modifiers to tailor the interactions between nanocolloids that could allow control of the degree of colloid stability for a wide variety of applications. Such knowledge of the thermodynamics of nanoparticle-polymer systems can lead to the development of *rational* manufacturing techniques necessary for reliable fabrication of nanostructures and materials. Such novel processes can be used to fabricate multi-dimension devices and composite nanomaterials from nanoscale components. Nanoscale devices and nanomaterials have the potential for new applications in all fields of science, from building smaller and more complex electronic circuits to creating highly selective and efficient catalysts for chemical and energy production. The ability of tailoring materials at the molecular level will affect industries such as microelectronics, pharmaceutical, chemical, biomedical and energy production by creating new commercially viable products such as paint and anti-corrosion compounds or by developing novel applications in drug delivery, biological implants, and prostheses.

The EEMC method extended for higher polymer concentrations for a nanocolloid in a freely adsorbing polymer solution showed that in general, μ_c decreases with increasing ρ_p and seems to be approaching a minimum, while Γ increases with ρ_p. The observed decrease in μ_c at higher ρ_p is due to polymer adsorption which increases with ρ_p.

Similar trends as compared to the work by Marla and Meredith[18] for dilute polymer concentrations were observed leading to the conclusion that ρ_p does not change the dependence of μ and Γ on n and σ_c.

The PLJC extended for the nanoparticle-polymer system and mPLJC EOS modified with a correction term that takes into account energetically asymmetric cases ($\varepsilon_{cs} < \varepsilon_{pp}$) showed very good agreement with EEMC simulation results for all n, ρ_p, and σ_c. The PLJC's shortcoming for energetic asymmetric cases is most likely due to μ^* dependence on the polymer-colloid excluded volume when the strength of attraction is diminished. The addition of a semi-empirical term in the mPLJC was able to predict satisfactorily the simulation results for all cases. The mPLJC was fitted to μ^* values from membrane osmometry experiments for aqueous PEO-silica dispersions. Deviations from experiments are most likely due to the v_p dependence on C_{si}.

The particle chemical potentials calculated from osmotic pressure were reported for an aqueous PEO-colloidal silica system in the range of 298-314 K. Chemical potential decreases, passes through a minimum, and increases again as PEO and silica concentration increases. This trend agrees qualitatively very well with EEMC simulation results. The minimum in μ versus v_{PEO} or v_{si} is due to the competing effects of entropy (due to the repulsive excluded volume interactions at high concentrations) and enthalpy (due to the attractive interactions and adsorption of polymer). This suggests the existence of an optimum polymer concentration for the minimization of the free energy. The effect of temperature on chemical potential also agrees well with EEMC simulation results. Temperature effects on the chemical potential were shown to increase chemical potential

with increasing T, due mostly to the negative effects of T on the adsorption of PEO onto silica.

In conclusion, simulation and experimental methods have been presented for the calculation of chemical potentials. In particular, the EEMC simulation study showed that polymer adsorption is a significant variable that determines if repulsive or attractive interactions dominate as evidenced by the decrease (attractive) or increase (repulsive) in μ with ρ_p. This result may lead to further understanding the importance of adsorbed polymer layers on the stability and self assembly of nanoparticles. Further work should be focused on studying the effects of adding particle-particle interactions by increasing the colloid concentration on the system. Furthermore, this study should be extended to the semi-dilute and dense regimes for both polymer and nanoparticles concentrations leading to the necessary knowledge required to predict phase behavior. The technique for using osmometry to measure the chemical potential may provide further insight into the molecular environment of nanocolloid-polymer mixtures to develop accurate equations of state and phase behavior predictions. Further research using this osmometry technique should be performed with additional colloid-polymer (CP) model systems that have been studied extensively such as poly(styrene) (PS)-silica in toluene and PS-poly (methylmethacrylate) (PMMA) in cis-decalin in order to extend this technique to non-adsorbing systems as well as to strengthen its validity. Measurement of chemical potential using osmometry to complement knowledge from simulation efforts can be used to scrutinize the effectiveness of surface passivating and stabilizing layers used in nanoparticle synthesis and self assembly essential to future nanotechnology applications.

REFERENCES

1. Chiew, Y., Lee, Y. & Rangaiah, G. A perturbed Lennard-Jones chain equation of state for polymer mixtures: applications to vapor-liquid and liquid-liquid equilibria. *Fluid Phase Equilib.* **189**, 135-150 (2001).

2. Shipway, A. N., Katz, E. & Willner, I. Nanoparticle arrays on surfaces for electronic, optical and sensor applications. *CHEMPHYSCHEM* **1**, 18-52 (2000).
3. Witten, T. & Pincus, P. *Macromolecules* **19**, 2509 (1986).

4. Kowalewski, T., McCullough, R. D. & Matyjaszewski, K. Complex nanostructured materials from segmented copolymers prepared by ATRP. *Eur. Phys. J. E* **10**, 5-16 (2003).

5. Murray, C. B., Kagan, C. R. & Bawendi, M. G. Self-organization of CdSe nanocrystallites into three-dimensional quantum dot superlattices. *Science* **270**, 1335-1338 (1995).

6. Kulkarni, G. U., Thomas, P. J. & Rao, C. N. R. Mesoscale organization of metal nanocrystals. *Pure Appl. Chem.* **74**, 1581-1591 (2002).

7. Choo, H. P., Liew, K. Y. & Liu, H. Factors affecting the size of polymer stabilized Pd Nanoparticles. *J. Mater. Chem.* **12**, 934-937 (2002).

8. Adachi, E. Three-Dimensional Self-Assembly of Gold Nanocolloids in Spheroid Due to Dialysis in the Presence of Sodium Mercaptoacetate. *Langmuir* **16**, 6460-6463 (2000).

9. Aubouy, M. & Raphael, E. Scaling description of a colloidal particle clothed with polymers. *Macromolecules* **31**, 4357-4363 (1998).

10. Sear, R. P. & Frenkel, D. Phase behavior of colloid plus polydisperse polymer mixtures. *Phys. Rev. E* **55**, 1677-1681 (1997).

11. Nowicki, W. Structure and Entropy of a Long Polymer Chain in the Presence of Nanoparticles. *Macromolecules* **35**, 1424 - 1436 (2002).

12. Fuchs, M. & Schweizer, K. S. Structure of colloid-polymer suspensions. *J. Phys.: Condens. Matter* **14**, R239-R269 (2002).

13. Fuchs, M. & Schweizer, K. S. Structure and thermodynamics of colloid-polymer mixtures: a macromolecular approach. *Europhys. Lett.* **51**, 621 (2000).

14. Fuchs, M. & Schweizer, K. S. Macromolecular theory of solvation and structure in mixtures of colloids and polymers. *Phys. Rev. E: Stat., Nonlinear, Soft Matter Phys.* **64**, 021514 (2001).

15. Haronska, P. & Vilgis, T. On the conformation of non-adsorbing polymers in colloidal suspensions. *J. Chem. Phys* **107**, 7501-7511 (1997).

16. Meijer, E. J. & Frenkel, D. Colloids dispersed in polymer solutions. A computer simulation study. *J. Chem. Phys* **100**, 6873 (1994).

17. Meijer, E. J. & Frenkel, D. Computer simulation of colloid-polymer mixtures. *Physica A* **213**, 130-137 (1995).

18. Marla, K. T. & Meredith, J. C. Nanoscale Colloids in a Freely Adsorbing Polymer Solution: A Monte Carlo Simulation Study. *Langmuir* **20**, 1501-1510 (2004).

19. Ye, X., Tong, P. & Fetters, L. Neutron Scattering Study of Colloidal Interactions in an Adsorbing Polymer Solution. *Macromolecules* **30**, 4103-4111 (1997).

20. Radosz, M. & Huang, S. Equation of State for small, large, polydisperse, and associating molecules. *Ind. Eng. Chem. Res.* **29**, 2284-2294 (1990).

21. Radosz, M. & Huang, S. EEquation of State for samll, large, polydisperse, and associating molecules - Extension to Fluid Mixtures. *Ind. Eng. Chem. Res.* **30**, 1994-2005 (1991).

22. Shen, S. & Lu, B. A Simple Perturbed Equation of State from a Pseudopotential Function. *Fluid Phase Equilib.* **84**, 9-22 (1993).

23. Song, Y., Lambert, S. & Prausnitz, J. M. Theta-Conditions in Binary and Multicomponent Polymer-Solutions using a Perturbed Hard-Sphere-Chain Equation of State. *Macromolecules* **28**, 4866-4876 (1995).

24. Song, Y., Lambert, S. & Prausnitz, J. M. A Perturbed Hard-Sphere-Chain Equation of State for Normal Fluids and Polymers. *Ind. Eng. Chem. Res.* **33**, 1047-1057 (1994).

25. Tochigi, K., Kurita, S. & Matsumoto, T. Prediction of PVT and VLE in polymer solutions using a cubic-perturebed equation of state. *Fluid Phase Equilib.* **158**, 313-320 (1999).

26. Prausnitz, J. M., Hino, T. & Song, Y. Liquid-liquid equilibria and theta temperatures in binary solvent-copolymer solutions from a perturbed hard-sphere-

chain equation of state. *J. Polym. Sci., Part B: Polym. Phys.* **34**, 1977-1985 (1996).

27. Chiew, Y., Chang, D., Lai, J. & Wu, G. A molecular-based equation of state for simple and chainlike fluids. *Ind. Eng. Chem. Res.* **38**, 4951-4958 (1999).

28. O'Lenick, R. & Chiew, Y. Variational Theory for Lennard-Jones Chains. *Mol. Phys.* **85**, 257-269 (1995).

29. von Solms, N., Chiew, Y. & O'Lenick, R. Lennard-Jones chain mixtures: variational theory and Monte Carlo simulation results. *Mol. Phys.* **96**, 15-29 (1999).

30. Cosgrove, T., Griffiths, P. C. & Lloyd, P. Polymer Adsorption. The Effect of the Relative Sizes of Polymer and Particle. *Langmuir* **11**, 1457-1463 (1995).

31. Cosgrove, T., Mears, S. J., Obey, T., Thompson, L. & Wesley, R. D. Polymer, particle, surfactant interactions. *Colloids Surf., A* **149**, 329-338 (1999).

32. Cosgrove, T., Jack, K. S., Nelson, A. & Kosak, D. NMR Solvent relaxation in Studies of Multicomponent Polymer Adsorption. *Langmuir* **18**, 2750-2755 (2002).

33. Mubarekyan, E. & Santore, M. M. Energy Barrier to Self-Exchange between PEO Adsorbed on Silica and solution. *Macromolecules* **34**, 7504-7513 (2001).

34. Zhang, Q. & Archer, L. A. Poly(ethylene oxide)/Silica Nanocomposites: Structure and Rheology. *Langmuir* **18**, 10435-10442 (2002).

35. Zhang, Q. & Archer, L. A. Optical Polarimetry and Mechanical Rheometry of Poly(ethylene oxide) - silica dispersions. *Macromolecules* **37**, 1928-1936 (2004).

36. Cosgrove, T., Fleer, G. J., Cohen Stuart, M. A., Scheutjen, J. M. H. M. & Vincent, B. *Polymer at Interfaces* (Chapman and Hall, London, 1993).

37. Quant, C. A. & Meredith, J. C. Measurement of Organically-Modified Nanoparticle Chemical Potentials using Osmometry. *Nanolett* **Submitted for Publication** (2004).

38. Escobedo, F. A. & de Pablo, J. J. Extended continuum configurational bias Monte Carlo methods for simulation of flexible molecules. *J. Chem. Phys.* **102**, 2636-2652 (1995).

39. Escobedo, F. & de Pablo, J. J. Monte Carlo simulation of the chemical potential of polymers in an expanded ensemble. *J. Chem. Phys.* **103**, 2703-2710 (1995).

40. Lyubartsev, A. P., Martsinovski, A. A., Shevkunov, S. V. & Vorontsov-Velyaminov, P. N. New approach to Monte Carlo calculation of the free energy: Method of expanded ensembles. *J. Chem. Phys* **96**, 1776-1783 (1992).

41. Wilding, N. B. & Muller, M. Accurate measurements of the chemical potential of polymeric systems by Monte Carlo simulation. *J. Chem. Phys* **101**, 4324 (1994).

42. Marla, K. T. & Meredith, J. C. Simulation of nanocolloid chemical potentials in a hard-sphere polymer solution: Expanded ensemble Monte Carlo. *J. Chem. Phys* **117**, 5443-5451 (2002).

43. Chiew, Y. Percus-Yevick integral-equation theory for athermal hard-sphere chains, Part I: Equations of state. *Mol. Phys.* **70**, 129-143 (1990).

44. Escobedo, F. & de Pablo, J. J. Expanded grand canonical and Gibbs ensemble Monte Carlo simulation of polymers. *J. Chem. Phys.* **105**, 4391-94 (1996).

45. Lu, Y. et al. Self-assembly of mesoscopically ordered chromatic polydiaceteylene/silica nanocomposites. *Nature* **410** (2001).

46. Israelachvili, J. N. *Intermolecular & Surface Forces* (Academic Press, San Diego, 1991).

47. Henderson, D., Duh, D.-M., Chu, X. & Wasan, D. An expression for the dispersion force between colloidal particles. *J. Colloid Interface Sci.* **185**, 265-268 (1997).

48. Metropolis, N., Rosenbluth, A. W., Rosenbluth, M. N., Teller, A. H. & Teller, E. Equation of state calculations by fast computing machines. *J. Chem. Phys* **21**, 1087-1092 (1953).

49. de Pablo, J. J., Laso, M., Suter, U. W. & Cochran, H. D. Continuum configurational bias Monte-Carlo studies of alkanes and polyethylene. *Fluid Phase Equilib.* **83**, 323-331 (1993).

50. Kumar, K. S., Szleifer, I. & Panagiotopoulos, A. Z. Determination of the Chemical potentials of polymeric systems from Monte Carlo Simulations. *Phys. Rev. Lett.* **66**, 2935-2938 (1991).

51. Escobedo, F. & de Pablo, J. J. Chemical potential and chain dimensions of chain molecules in athermal environments. *Mol. Phys.* **89**, 1733-1754 (1996).

52. Widom, B. Some topics in theory of fluids. *J. Chem. Phys* **39**, 2808-2812 (1963).

53. Shing, K. S. & Gubbins, K. E. The chemical potential from computer simulation. Test particle method with umbrella sampling. *Mol. Phys.* **43**, 717--721 (1981).

54. Escobedo, F. A. & de Pablo, J. J. A new method for generating volume changes in isobaric-isothermal Monte Carlo simulations of flexible molecules. *Macromol. Theory Simul.* **4**, 691-707 (1995).

55. Siepmann, J. I. A method for the direct calculation of chemical potentials for dense chain systems. *Mol. Phys.* **70**, 1145-1158 (1990).

56. Mooij, G. C. A. M. & Frenkel, D. Novel scheme to compute chemical potentials of chain molecules on a lattice. *Mol. Phys.* **74**, 41-47 (1991).

57. Allen, M. P. & Tildesley, D. J. *Computer Simulation of Liquids* (Oxford University Press, Clarendon,Oxford, 1987).

58. Chiew, Y. & O'Lenick, R. Lennard-Jones chain mixtures: radial distribution functions from Monte Carlo simulation. *Mol. Phys.* **97**, 997-1008 (1999).

59. Hino, T., Song, Y. & Prausnitz, J. M. Liquid-liquid equilibria and theta temperatures in homopolymer-solvent solutions from a perturbed hard-sphere-chain equation of state. *J. Polym. Sci., Part B: Polym. Phys.* **34**, 1961-1976 (1996).

60. Flory, P. J. *Statistical Mechanics of Chain Molecules* (Hanser Publishers, New York, 1988).

61. Oesterhelt, F., Rief, M. & Gaub, H. Single molecule force spectroscopy by AFM indicates helical structure of poly(ethylene-glycol) in water. *New J. Phys* **1**, 6.1-6.11 (1999).

62. Cho, J. & Sanchez, I. C. An Analytical Free Energy and the Temperature Pressure Superposition Principle in Pure Polymeric Liquids. *Macromolecules* **31**, 6650-6661 (1998).

63. Helfer, C. A., Xu, G., Mattice, W. L. & Pugh, C. Monte Carlo SImulation Investigating the Threading of Cyclic Poly(ethylene oxide) by linear chains in the melt. *Macromolecules* **36**, 10071-10078 (2003).

64. Gai, F., Lu, Q. & Zhao, D. Controllable assembly of Ordered Semiconductor Ag2S Nanostructures. *Nano Lett.* **3**, 85 (2002).

65. Liu, Z. et al. Organization of nanoparticles on soft polymer surfaces. *Nano Lett.* **2**, 219-224 (2002).

66. Atkins, P. & de Paula, J. *Phys. Chem.* (W.H. Freeman, New York, 2002).

67. Flory, P. J. *Principles of Polymer Chemistry* (Cornell University Press, Ithaca, 1953).

68. Tompa, H. *Polymer Solutions* (Academic Press, New York, 1956).

69. Prausnitz, J. M., Lichtenthaler, R. N. & Gomes de Azevedo, E. *Molecular Thermodynamics of Fluid-Phase Equilibria* (ed. Amundson, N.) (Prentice Hall, Upper Saddle River, 1999).

70. Lekkerkerker, H. N. W. Osmotic Equilibrium Treatment of the Phase Separation in Colloidal Dispersions Containing Non-adsorbing polymer molecules. *Colloids Surf., A* **51**, 419-426 (1990).

71. Quant, C. A. & Meredith, J. C. Expanded Ensemble Monte Carlo Simulation of Attractive Nanocolloid-Polymer Mixtures: Comparison to a Modified Perturbed Lennard-Jones Equation of State. *Langmuir* **Submitted for Publication** (2004).

72. Wind, B. & Killmann, E. Adsorption of poly(ethylene oxide) on surface-modified silica. Stability of bare and covered particles in suspension. *Colloid Polym. Sci.* **276**, 903-912 (1998).

73. Cosgrove, T., Mears, S. J., Thompson, L. & Howell, I. Solvent Relaxation NMR Measurements on Polymer particle, Surfactant Systems. *Langmuir* **14**, 997-1001 (1998).